Copy No. 1

RM No. A7F09

NACA RM No. A7F09

RESEARCH MEMORANDUM

A SUMMARY AND ANALYSIS OF DATA ON DIVE-RECOVERY FLAPS

By Lee E. Boddy and Walter C. Williams

Ames Aeronautical Laboratory
Moffett Field, Calif.

NATIONAL ADVISORY COMMITTEE
FOR AERONAUTICS

WASHINGTON

September 9, 1947

RM No. A7F09

NATIONAL ADVISORY COMMITTEE FOR AERONAUTICS

RESEARCH MEMORANDUM

A SUMMARY AND ANALYSIS OF DATA ON DIVE-RECOVERY FLAPS

By Lee E. Boddy and Walter C. Williams

SUMMARY

The results of numerous unrelated tests of dive-recovery flaps are collected in this report and presented in a form suitable for use in the preliminary design of dive-recovery flap installations. Since the data were obtained for airplane models of quite widely varying configurations, and are limited largely to a Mach number of 0.80, it is recommended that each new installation be carefully flight-tested before final approval. A flight-test procedure is outlined which will insure a maximum degree of safety.

INTRODUCTION

Considerable difficulty has been experienced with many modern conventional airplanes in recovering from high-speed dives. As a result, various corrective devices have been investigated, the most successful of which has been the dive-recovery flap. This device is a small split flap mounted on the lower surface of the airplane wing. A typical installation on a wind-tunnel model is shown in figure 1, and an experimental installation on an airplane for flight tests is shown in figure 2.

Dive-recovery flaps were tested first in the Ames 16-foot high-speed wind tunnel in October 1942, and were first tested in flight by the Lockheed Aircraft Corporation from December 1942 to April 1943. Subsequent flight tests were made by the Army Air Forces and the Republic Aviation Corporation with a Republic P-47 airplane and by the Langley Memorial Aeronautical Laboratory with a North American XP-51 airplane. More recently the Ames 16-foot high-speed wind tunnel has tested dive-recovery flaps on a number of airplane models in conjunction with more general investigations.

It is the purpose of this report to collect all the available

data on the subject and present them in a form which will serve as a guide for the preliminary design of dive-recovery flaps. By necessity, many factors pertaining largely to airplane configuration have been ignored. Consequently, a flight-test procedure is recommended. It is believed that the data presented herein, if used in conjunction with the recommended flight-test procedure, will facilitate the developement of satisfactory dive-recovery-flap installations for most conventional airplanes.

SYMBOLS

The following symbols are used in this report:

General

V free-stream velocity, feet per second

ρ free-stream mass density, slugs per cubic foot

q free-stream dynamic pressure ($\frac{1}{2}\rho V^2$), pounds per square foot

M Mach number $\left(\frac{V}{\text{velocity of sound}}\right)$

ΔM increase of Mach number over that for lift divergence

P pressure coefficient $\left[\frac{(\text{local static pressure})-(\text{free-stream static pressure})}{q}\right]$

P_{cr} critical pressure coefficient (P at which the local velocity equals the local velocity of sound)

g acceleration of gravity, feet per second per second

ΔH decrease of total pressure from free-stream total pressure, pounds per square foot

Airplane or Model Dimensions

S wing area, square feet

S_f total flap area, square feet

b wing span, feet

b_f total flap span, feet

b_e elevator span, feet

M.A.C. wing mean aerodynamic chord, feet

c_w average wing chord at the flap, feet

c_f average flap chord, feet

$\overline{c_e^2}$ mean-square elevator chord, square feet

x longitudinal distance from the wing leading edge, feet

Coefficients

C_L lift coefficient $\left(\frac{\text{lift}}{qS}\right)$

C_m pitching-moment coefficient $\left(\frac{\text{pitching moment}}{qS \text{ M.A.C.}}\right)$

ΔC_m increase of pitching-moment coefficient for constant lift coefficient due to the flaps

ΔC_{m_w} increase of wing pitching-moment coefficient for constant lift coefficient due to the flaps

ΔC_D increase of drag coefficient due to the flaps $\left(\frac{\text{increase of drag}}{qS}\right)$

C_{h_e} elevator hinge-moment coefficient $\left(\frac{\text{elevator hinge moment}}{q\ \overline{c_e^2}\ b_e}\right)$

Angles

α airplane or model angle of attack, degrees

α_u uncorrected angle of attack, degrees

$\Delta\alpha$ increase of angle of attack for constant lift coefficient due to the flaps, degrees

α_t airplane or model tail angle of attack, degrees

$\Delta\alpha_t$ increase of tail angle of attack at constant lift coefficient due to the flaps, degrees

δ_f flap deflection, degrees

δ_e elevator deflection, degrees

$\Delta\delta_{e_0}$ increase of elevator floating angle due to the flaps, degrees

RESULTS

Source of Data

The wind-tunnel data collected in this report are the results of numerous unrelated tests conducted in the Ames 16-foot high-speed wind tunnel from October 1942 to June 1945. Several improvements of the model support system were made during this period, particularly with regard to increasing its critical Mach number and reducing its interference at high Mach numbers. Although all the data have been recently corrected for tares, constriction, and flow inclination due to the support system according to latest knowledge, some discrepancies may be present because of the varying interference of different support systems and different flap positions relative to the supports.

The flight data are the results of tests conducted by the Langley Laboratory.

Presentation of Results

Basic data.- The effect of dive-recovery flaps on the lift and pitching-moment characteristics of the models tested in the wind tunnel is shown in figures 3 to 14. Included in each figure is a half plan view of the model as well as pertinent geometrical information on the flap installation. Additional information concerning the behavior of the flaps may be gained from figures 15 and 16, which show the effect of typical installations on the wing chordwise pressure distribution and on the wing wake at the horizontal tail plane. The drag coefficient due to all the flaps tested is summarized in figure 17 for the purpose of determining their effect on the velocity of the airplane. It should be noted that the drag

coefficient of each installation was divided by the ratio of projected flap frontal area to wing area in order to account for different flap sizes on the various models.

Flap effectiveness.- Although the purpose of the dive-recovery flaps on a particular airplane is to increase its trim lift coefficient, it is most convenient to consider flap effectiveness as the increase of pitching-moment coefficient at a given lift coefficient. By so doing, the effect of center-of gravity position is eliminated. Furthermore, in order to reduce the data to a form suitable for general application, it is necessary to consider not the total pitching moment increment but the individual contributing factors. These are (1) the effect on the wing pitching-moment characteristics, and (2) the effect on the tail lift (or pitching moment due to the tail). The second factor may be attributed mainly to a change of tail angle of attack and a change of elevator floating angle. (The results indicate that changes of tail efficiency are small and may be neglected.) Therefore the total pitching-moment coefficient due to the flaps may be represented by the following equation:

$$\Delta C_m = \Delta C_{m_W} + \Delta\alpha_t \left(\frac{\partial C_m}{\partial \alpha_t}\right)_\alpha + \Delta\delta_{e_O} \left(\frac{\partial C_m}{\partial \delta_e}\right)_{\alpha_t}$$

In turn, the change of tail angle of attack may be attributed to a change of airplane angle of attack for a given lift coefficient and to a change of downwash at the tail due to the altered spanwise distribution of lift with the flaps deflected. Both are dependent upon the lift developed by the flaps. Hence, the change of tail angle of attack may be represented by the product of (1) the change of airplane angle of attack for a given lift coefficient, which is largely a function of the size and chordwise location of the flaps, and (2) the ratio of change of tail angle of attack to change of airplane angle of attack, which is mainly a function of spanwise location of the flaps. Therefore,

$$\Delta C_m = \Delta C_{m_W} + \Delta\alpha \left(\frac{\Delta\alpha_t}{\Delta\alpha}\right)\left(\frac{\partial C_m}{\partial \alpha_t}\right)_\alpha + \Delta\delta_{e_O} \left(\frac{\partial C_m}{\partial \delta_e}\right)_{\alpha_t} \qquad (1)$$

Also, if the elevator characteristics are linear within the range being considered, and it is assumed that the change of elevator floating angle is attributable mainly to the change of tail angle of attack,

$$\Delta\delta_{e_O} = -\frac{\left(\frac{\partial C_{h_e}}{\partial \alpha_t}\right)_{\delta_e}}{\left(\frac{\partial C_{h_e}}{\partial \delta_e}\right)_{\alpha_t}}\left(\frac{\Delta\alpha_t}{\Delta\alpha}\right)\Delta\alpha$$

and

$$\Delta C_m = \Delta C_{m_W} + \Delta\alpha\left(\frac{\Delta\alpha_t}{\Delta\alpha}\right)\left[\left(\frac{\partial C_m}{\partial \alpha_t}\right)_\alpha - \frac{\left(\frac{\partial C_{h_e}}{\partial \alpha_t}\right)_{\delta_e}\left(\frac{\partial C_m}{\partial \delta_e}\right)_{\alpha_t}}{\left(\frac{\partial C_{h_e}}{\partial \delta_e}\right)_{\alpha_t}}\right] \qquad (2)$$

It should be remembered that the change of tail angle of attack considered here is an average along the span of the tail, and equation (2) is applicable only if the tail characteristics are essentially constant along the span.

Values of ΔC_{m_W}, $\Delta\alpha$, and $\Delta\alpha_t/\Delta\alpha$ were computed for each flap installation tested and are given in figures 18 to 21, since all other factors in the foregoing equation are characteristics of the particular airplane and not of the flaps. Since most of the flaps were tested at several deflections, plots were first made of $\Delta\alpha$ against the ratio of projected flap frontal area to wing area and of ΔC_{m_W} against the ratio of the product of the projected flap frontal area and wing chord at the flap to the product of wing area and mean aerodynamic chord (such as the example in fig. 18). An average linear variation throughout the usable range was assumed as indicated by the dashed lines in the example; the slope of these lines was then taken as the effectiveness of the flaps and plotted against Mach number in figure 19. Values are shown for lift coefficients of 0.00 and 0.40, corresponding to typical conditions for a vertical dive and for moderate recovery from a high-speed dive. In figure 20 the effectiveness is shown as a function of chordwise location of the flaps for constant values of Mach number relative to the Mach number of lift divergence. However, it should be remembered that the results are for models having quite varied configurations, and the effects shown may not be due entirely to chordwise location. Complete data for flaps at various chordwise positions on the same model are available only for the YP-80A model, and the curves shown in figure 20 are faired through the data obtained for this model.

Figure 21 shows a front view of each installation tested and the corresponding values of $\Delta\alpha_t/\Delta\alpha$. (Plots were first made of $\Delta\alpha_t/\Delta\alpha$ which revealed no appreciable variation with flap deflection.) Figures 22 and 23 show typical effects of flaps on the elevator characteristics. Figure 24 presents the results of flight tests made with a small airfoil mounted in the high-speed-flow region of the airplane wing in order to obtain qualitative information concerning the effectiveness of dive-recovery flaps at Mach numbers near 1.0.

Although it is realized that many secondary factors (such as airfoil section, wing aspect ratio, and support interference) influence the effectiveness, it is impossible to completely determine their magnitude from the data at hand. For this reason, it is desirable that each new installation be carefully flight-tested before final approval. Figure 25 shows the results of such a test.

DISCUSSION

General Behavior of Dive-Recovery Flaps

Flap deflection.- All the flaps tested were well forward of the wing trailing edge and exhibited the general characteristics of spoilers. For low Mach numbers the small deflections were relatively ineffective and in some cases had reversed effectiveness. For high Mach numbers, however, the reversal tended to disappear, and for practical purposes the effectiveness may be assumed to vary linearly with the projected flap frontal area. (See fig. 18.)

Mach number.- In general, the effectiveness of the flaps increased considerably with increasing Mach number to well past the Mach number of lift divergence. (See fig. 19.) As shown in the typical pressure distribution (fig. 15) the pressure recovery aft of the flap was less complete at high Mach numbers, causing a considerable increment of negative pressure over a large portion of the upper wing surface. Also, the upper-surface shock moved aft when the flaps were deflected. Both of these effects contributed to the flap effectiveness. However, there is evidence that the effectiveness will decrease sharply above some Mach number between that for lift divergence and a Mach number of 1.0. (See fig. 24.) Moreover, it is believed that the Mach number at which the flap effectiveness decreases will more closely approach the Mach number of lift divergence as the latter approaches a value of 1.0. It is important, then, that extreme caution be exercised in testing dive-recovery flaps on airplanes having a very high Mach number of lift

divergence.

It will be noted that the increment of wing pitching-moment coefficient due to the flaps became more negative as the Mach number increased. (See fig. 19.) This is due to the fact that the increase of Mach number caused an increase of flap effectiveness which was applied largely to the wing aft of the position of the upper-surface shock. In order to prevent serious changes of tail loads and a decrease of the total flap effectiveness, it is desirable that the change of wing pitching-moment coefficient be as small as possible.

Location on the wing.- In presenting the results it was assumed that the factors $\Delta\alpha$ and ΔC_{m_w} are predominantly affected by the size and chordwise location of the flaps on the wing, while the factor $\Delta\alpha_t/\Delta\alpha$ is largely a function of the spanwise location of the flaps. This assumption is based on simple theory and should be valid except for cases where three-dimensional effects are large (such as for flaps near the wing tip), or for installations which are greatly affected by interference of fuselage, nacelles, etc. Moreover, it should be noted that most of the wings tested were essentially unswept and the values of ΔC_{m_w} given in this report will not necessarily be correct for wings with considerable sweep. A swept-back wing with flaps inboard of the mean aerodynamic chord probably would exhibit more positive values of ΔC_{m_w}. Also, the effectiveness of the flaps probably would be less on highly swept wings due to the cross flow.

In general, the flaps located well forward on the chord of the wing were more satisfactory than those nearer the trailing edge. (See fig. 20.) The forward flaps produced a greater decrease of angle of attack for constant lift coefficient, and also caused smaller negative shifts of the wing pitching-moment coefficient. Large negative shifts of the wing pitching-moment coefficient should be avoided since they not only reduce the total effectiveness of the flaps but may cause serious increases of tail loads. However, there is a practical limit to the forward location of the flaps. The range of positive lift coefficients for which the forward flaps were effective was considerably smaller than that for the rearward flaps. (See fig. 5.) Also, the flaps in the more rearward positions maintained their effectiveness to a slightly higher Mach number than did those nearer the leading edge, especially at the higher lift coefficients. Apparently the flow behind the flaps which were well ahead of the lower-surface minimum-pressure point had a strong tendency to return to the wing surface. For this reason, dive-recovery flaps on airplanes requiring a high lift coefficient for dive recovery should be located farther aft than those on airplanes requiring

a lower lift coefficient. It appears that the optimum chordwise flap location for airplanes requiring approximately 0.40 lift coefficient is about one-third of the wing chord back of the leading edge.

The change of tail angle of attack $\Delta\alpha_t/\Delta\alpha$ is shown in figure 21 for all the flaps tested. Values of $\Delta\alpha_t/\Delta\alpha$ varied from about 0.8 for a model with the flaps completely outboard of the tail to about 2.0 for a twin-fuselage model with the flaps entirely in front of the tail. Typical values for flaps partially in front of the tail were between 0.9 and 1.2.

Wing section.- No comprehensive results are available which will show the effects of wing section on the behavior of dive-recovery flaps. It has already been mentioned that the chordwise position of the upper-surface shock might affect the wing pitching-moment coefficient due to the flaps, and that the chordwise position of the lower-surface minimum-pressure point probably affects the behavior of flaps located near the wing leading edge. Within the range used on airplanes at present, wing-thickness ratio must be accounted for inasmuch as it affects the Mach number of lift divergence.

Elevator characteristics.- In developing equation (2) of the section entitled "Results," it was assumed that the change of elevator floating angle due to the flaps arose from the change of tail angle of attack. This assumption is substantiated by the results shown in figures 22 and 23. The dive-recovery flaps did not greatly change the elevator floating angle of the model whose elevator hinge moments were essentially unaffected by changes of tail angle of attack (or airplane lift coefficient). However, a large change of elevator floating angle was noted for the model the elevator hinge moments of which varied considerably with tail angle of attack. At a Mach number of 0.70, the elevator hinge moments with the flaps deflected appeared to be about the same for a lift coefficient of 0.40 as they were with the flaps retracted for a lift coefficient of about -0.1. This indicates that the flaps decreased the tail angle of attack about 3.5° (using a measured value of 7.0° for $\partial\alpha_t/\partial C_L$). The lift and pitching-moment results (figs. 11, 19, and 21) indicate a decrease of tail angle of attack of 3.1° and 3.6° at lift coefficients of 0.00 and 0.40, respectively. In view of the absence of information for a wider range of models, the results are conclusive enough to justify the assumption.

It is significant that the flaps did not change the elevator effectiveness of the two models for which data are available. As a result, it can be assumed that the horizontal-tail effectiveness

would not be seriously affected, and flap-retracted values of $(\partial C_m/\partial \delta_o)_{\alpha_t}$ and $(\partial C_m/\partial \alpha_t)_\alpha$ may be used in the equations for total pitching-moment coefficient due to the flaps.

Structural and Mechanical Considerations

Flap loads.- Limited pressure-distribution measurements have been made on typical dive-recovery flaps which indicate a trapezoidal chordwise loading with a maximum loading at the hinge line. For practical design purposes a uniform chordwise loading may be used. Except for small deflections where the pressures might be reversed, the normal-force coefficient may be assumed to vary linearly with flap deflection to a value of 1.1 for a deflection of 45°.

Rate of flap deflection.- The flap actuating mechanism should be supplied with sufficient power to deflect the flaps rapidly. The rates of flap deflection for successful installations tested in flight have been such that full flap deflection was reached in 1 to 1½ seconds. Slower rates of deflection result in dangerous response lag and a consequent greater loss of altitude during recovery from a dive. In addition, the adverse effects of the flaps for small deflections are accentuated.

Buffeting.- It has been shown that the most effective spanwise location for dive-recovery flaps is directly in front of the horizontal tail. Although no conclusive data are available on the matter, there may be some danger of tail buffeting with flaps in this location. Therefore, a compromise spanwise location is recommended that places the flaps in front of only the outboard portions of the tail, especially on airplanes which do not have a particularly high tail position with respect to the wing. Also, isolated cases of wing buffeting have been reported with dive-recovery flaps deflected, wherein the landing flaps vibrated through a comparatively small amplitude. It is believed that this was due to a small amount of play in the landing-flap restraint mechanism.

Recommended Design Procedure

It has been shown that the effectiveness of dive-recovery flaps in increasing the pitching-moment coefficient of an airplane is maintained past the Mach number of lift divergence for the airplane. However, the trim lift coefficient and resultant acceleration are less at Mach numbers above that for lift divergence because of the increased static longitudinal stability. (See fig. 25.) Hence, a

successful dive-recovery flap installation is one which will effect sufficient (but not excessive) recovery of the airplane from a dive to any Mach number and altitude, which the airplane is capable of attaining, without causing undue stress on any part of the aircraft structure. The following procedure for the preliminary design of dive-recovery flaps for a particular airplane is offered:

1. Establish the Mach number, altitude, and lift coefficient at which the recovery is desired. (The drag due to the flaps may be neglected since appreciable changes of drag affect the velocity only slightly above the Mach number of lift divergence.)

2. Compute or estimate the elevator-free pitching-moment characteristics of the airplane with the normal center-of-gravity position for the above Mach number. From those characteristics determine the pitching-moment-coefficient increment necessary to trim the airplane at the lift coefficient of step 1.

3. Select a flap location on the wing which is structurally suitable for the airplane (around 30 or 40 percent of the chord and partially in front of the horizontal tail if possible).

4. Assume the flap size for a comparable installation from figures 3 to 14.

5. Compute values for $\Delta\alpha$, ΔC_{m_w}, and $\Delta\alpha_t/\Delta\alpha$ from figures 20 and 21 for the flap size assumed and a deflection of 30°. (This will allow some adjustment of the effectiveness during flight tests if necessary.)

6. Compute ΔC_m using the equations developed in the section entitled "Results." If the elevator characteristics are linear within the range being considered, equation (2) may be used; otherwise, the change of elevator floating angle should be determined directly from the elevator characteristics and equation (1) should be used.

7. If the ΔC_m computed in step 6 does not agree with that of step 2, repeat the procedure with a different flap size.

Once the flap size is established, it would be wise to compute the acceleration available from the flaps for all Mach numbers and altitudes which the airplane is capable of attaining, for both the most forward and the most rearward center-of-gravity position. Also, the tail loads with the flaps deflected should be checked if it

appears that the flap location chosen will result in an appreciable value of ΔC_{m_w}.

Recommended Flight-Test Procedure

In view of previously mentioned deficiencies of the available data, it is desirable that each new dive-recovery-flap installation be carefully flight-tested before final approval. A step-by-step procedure is recommended which consists of trimming the airplane for a given speed and deflecting the flaps. The stick-free condition should be simulated and the elevator control used only to prevent excessive accelerations. Measurements should be made of the Mach number and altitude at which the flaps are deflected and of the maximum acceleration obtained during the resulting maneuver.

Runs should be made throughout the speed range, but it is desirable that the first runs be made at comparatively low Mach numbers and high altitude in order to avoid excessive accelerations. A running record should be kept so that the flap effectiveness at the higher Mach numbers may be anticipated.

Particular care should be exercised in obtaining data above the Mach number of lift divergence for the airplane. The desired Mach number should be approached gradually at the minimum diving angle necessary to attain that Mach number at the altitude being used. As a result, the maximum Mach number of any particular run will be only slightly greater than the Mach number for which data have already been obtained. Following the above precautions will result in obtaining the necessary information with a maximum degree of safety.

CONCLUSIONS

An analysis of the data collected in this report indicates the following:

1. In order to obtain maximum effectiveness, as well as to avoid tail buffeting and large increases of tail loads, dive-recovery flaps should be located about one-third of the wing chord from the leading edge with part of the flap in front of the outboard portion of the horizontal tail.

2. All the flaps tested were effective above the Mach number of lift divergence for the airplane.

3. The flap effectiveness probably will become negligible at some Mach number between that of lift divergence for the airplane and a Mach number of 1.0.

4. All new dive-recovery-flap installations should be carefully flight-tested, especially those intended for use on airplanes with a very high Mach number of lift divergence.

Ames Aeronautical Laboratory,
National Advisory Committee for Aeronautics,
Moffett Field, Calif.

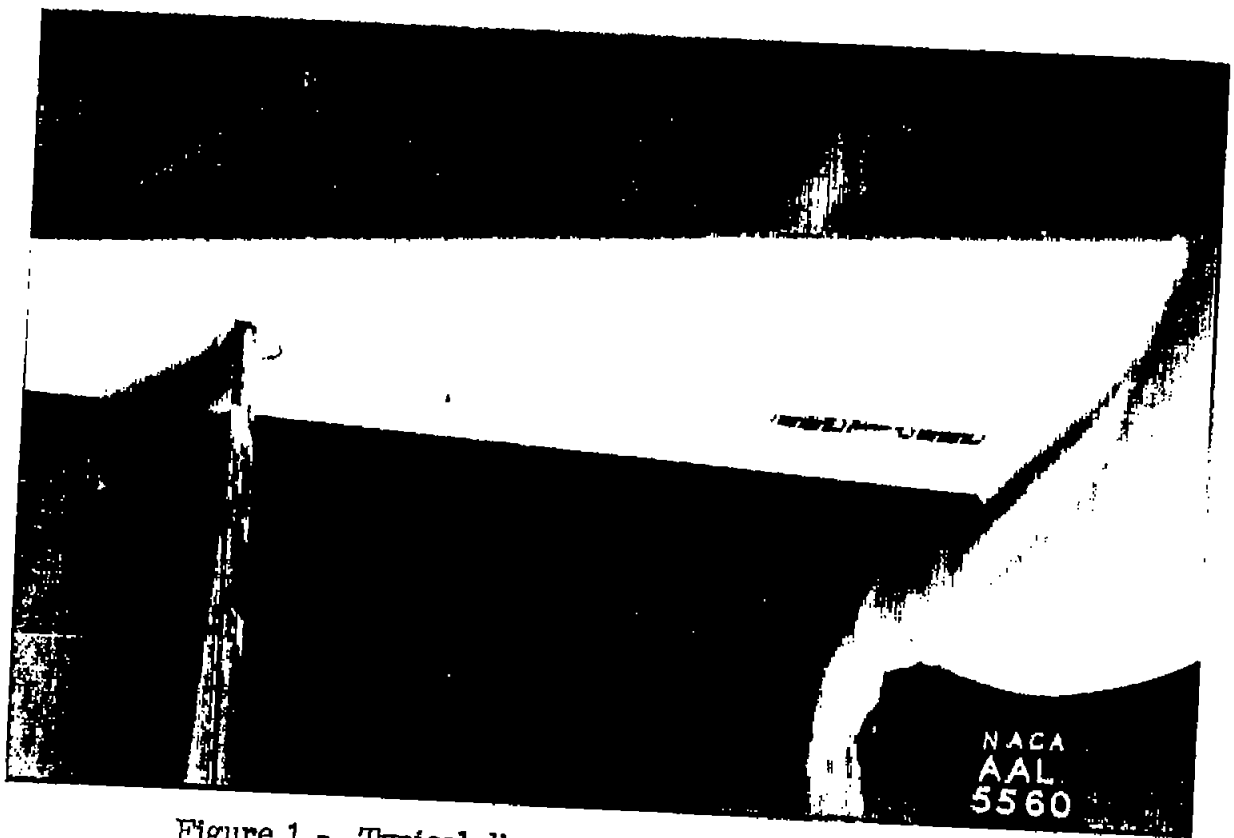

Figure 1.- Typical dive-recovery-flap installation on a wind-tunnel model.

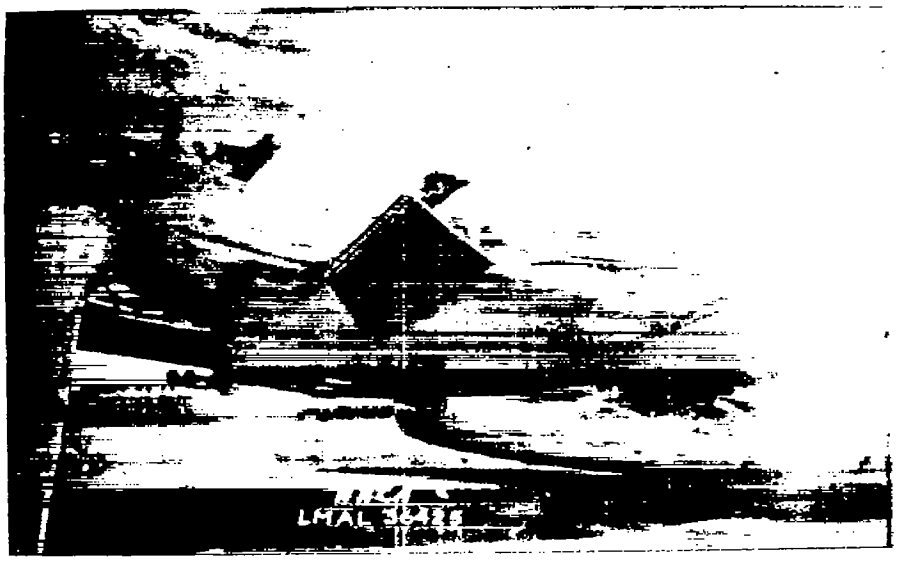

(a) Flap deflected 30°.

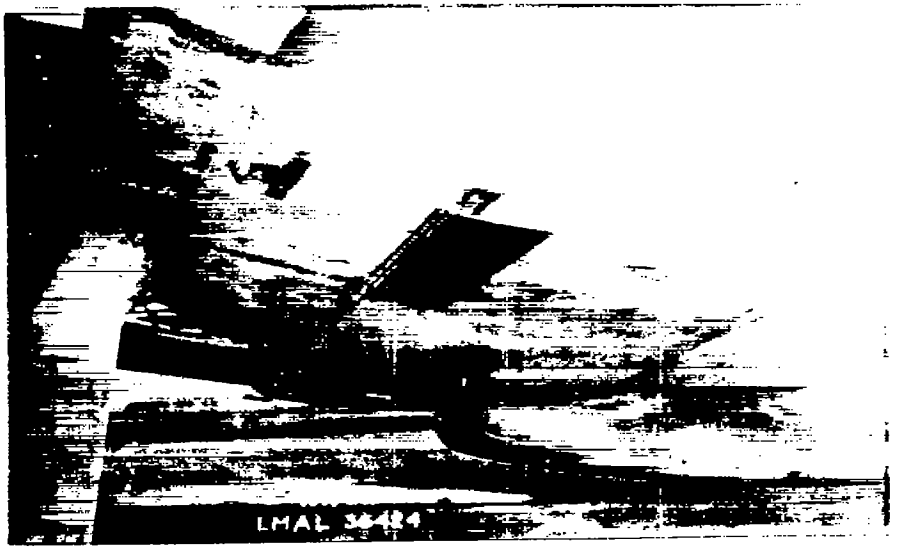

(b) Flap fully retracted.

Figure 2.- Dive-recovery flap located on left wing of the XP-51 airplane.

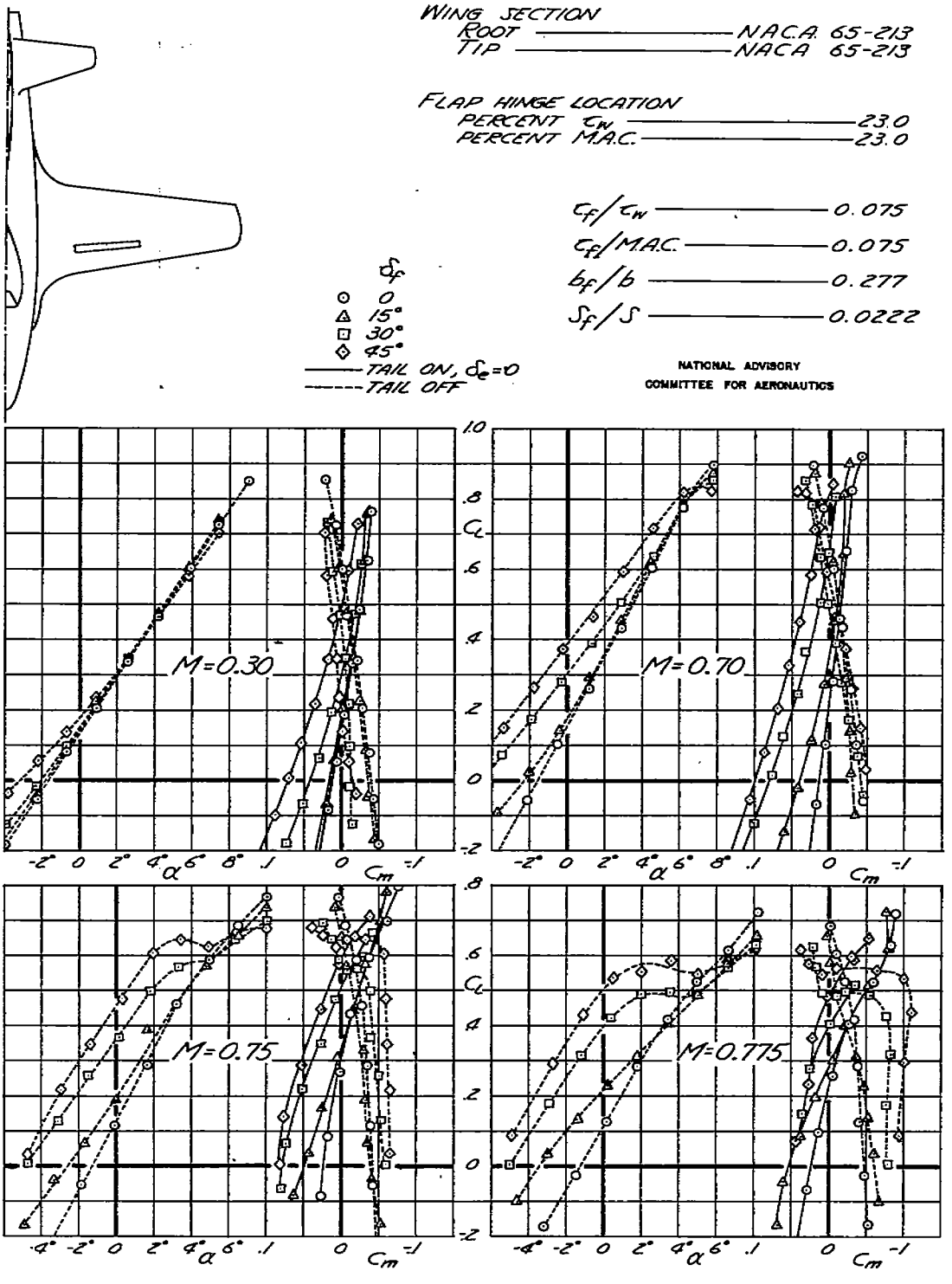

FIGURE 3.- EFFECT OF DIVE-RECOVERY FLAPS ON THE LIFT AND PITCHING-MOMENT CHARACTERISTICS OF THE LOCKHEED XP-80 AIRPLANE MODEL WITH AN NACA 65-213 WING.

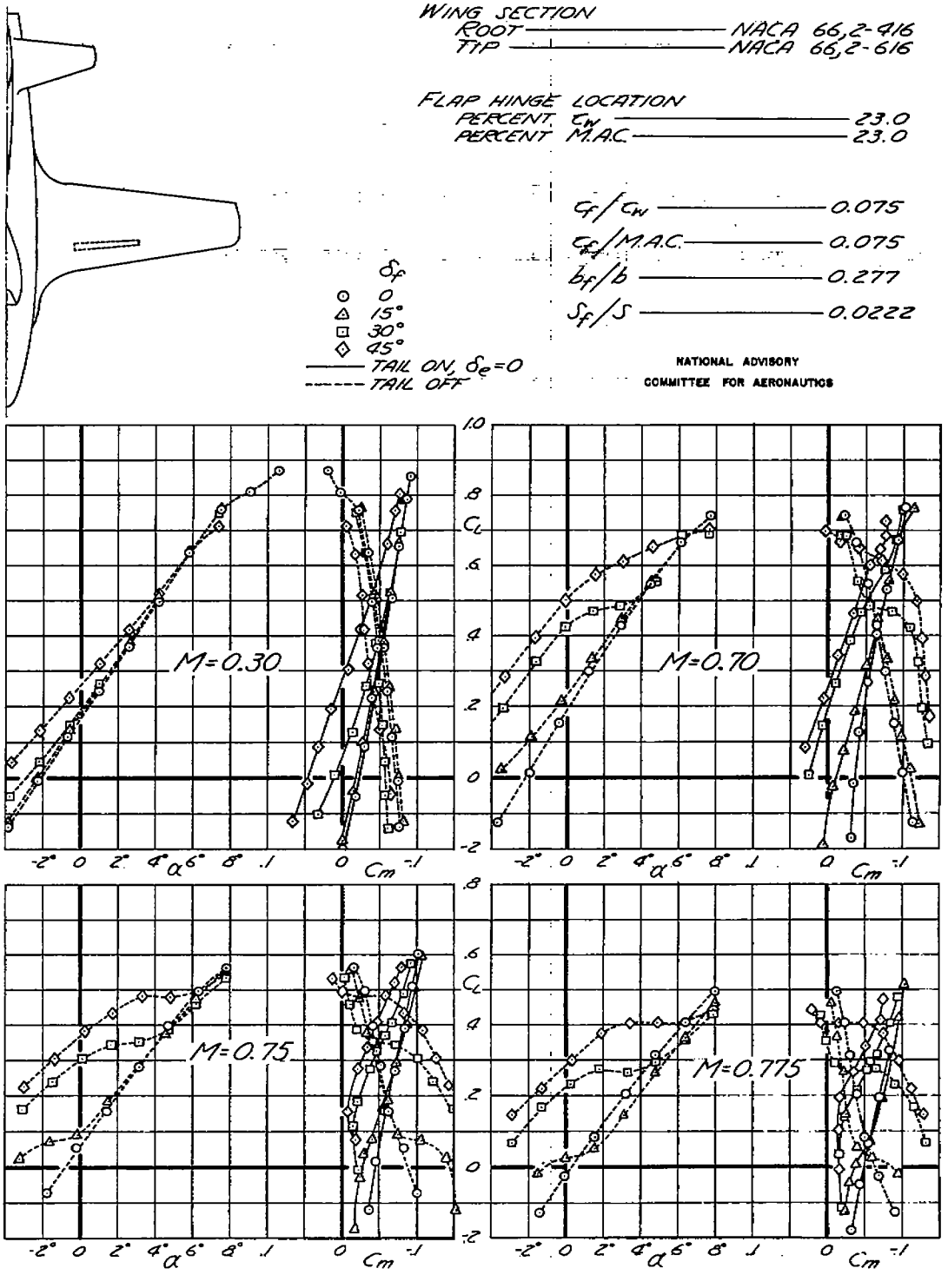

FIGURE 4.- EFFECT OF DIVE-RECOVERY FLAPS ON THE LIFT AND PITCHING-MOMENT CHARACTERISTICS OF THE LOCKHEED XP-80 AIRPLANE MODEL WITH A HIGHLY CAMBERED NACA 66-SERIES WING.

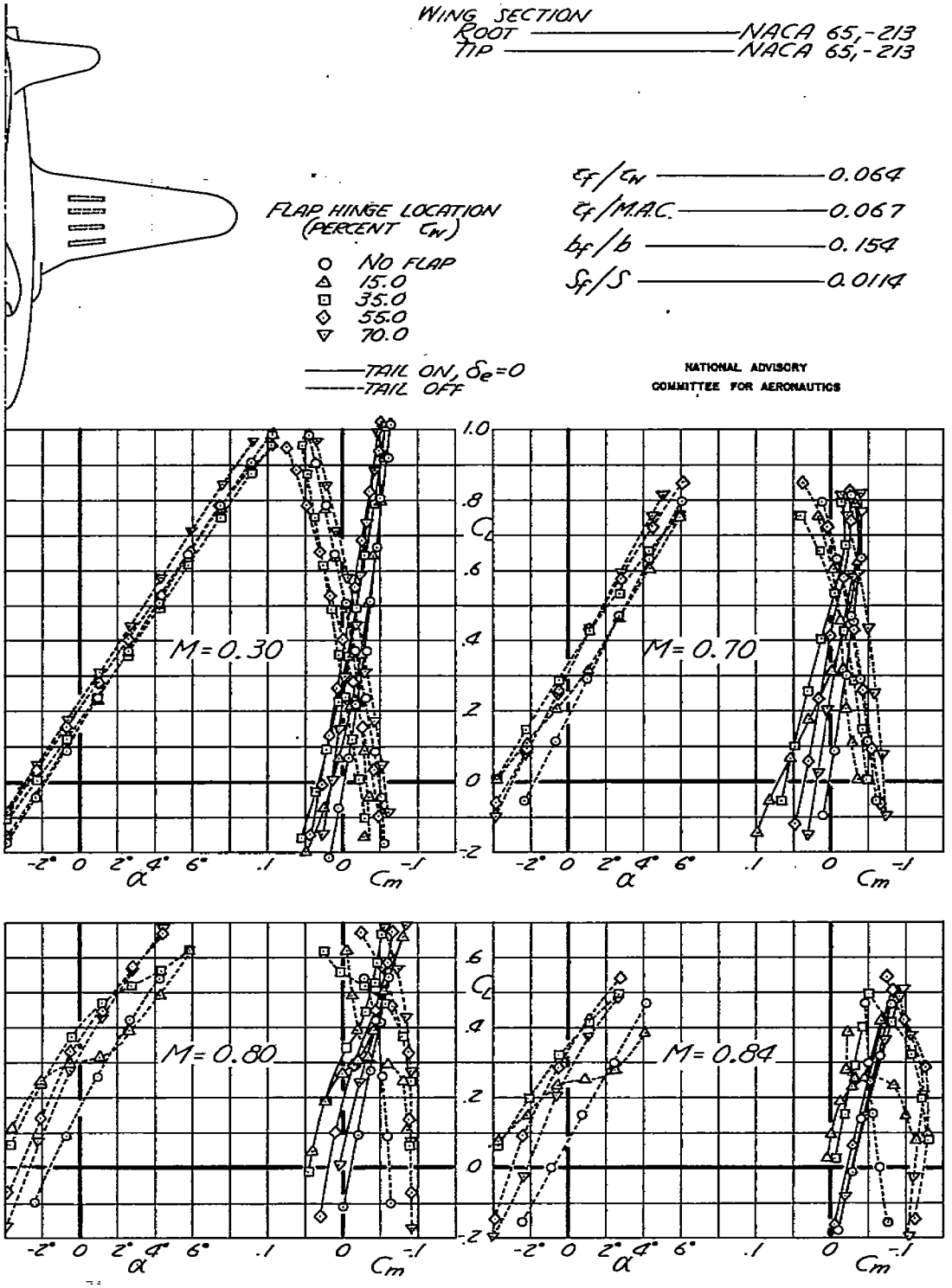

FIGURE 5.- EFFECT OF DIVE-RECOVERY FLAPS ON THE LIFT AND PITCHING-MOMENT CHARACTERISTICS OF THE LOCKHEED YP-80A AIRPLANE MODEL.

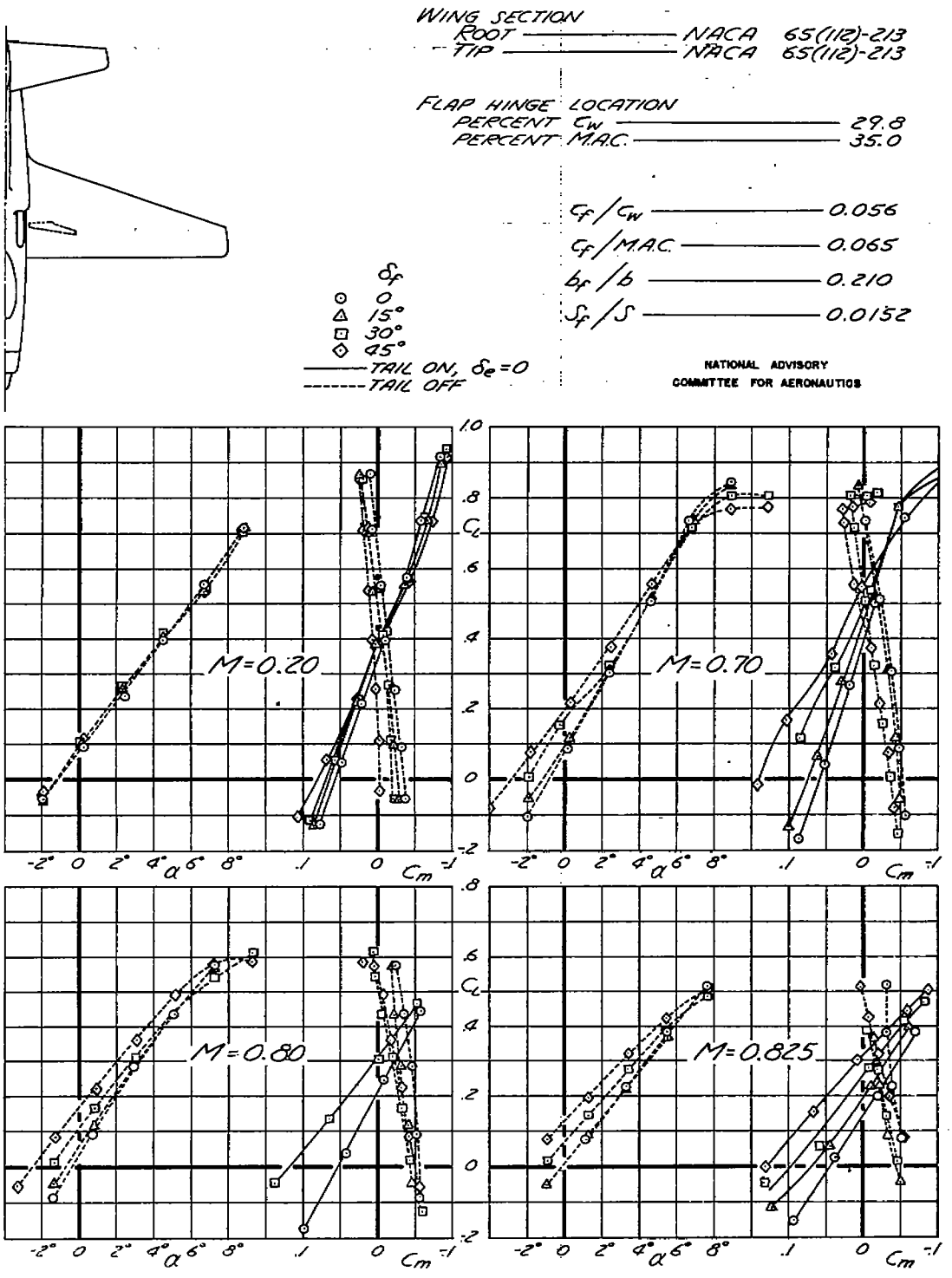

FIGURE 6. - EFFECT OF DIVE-RECOVERY FLAPS ON THE LIFT AND PITCHING-MOMENT CHARACTERISTICS OF THE CONSOLIDATED-VULTEE XP-81 AIRPLANE MODEL.

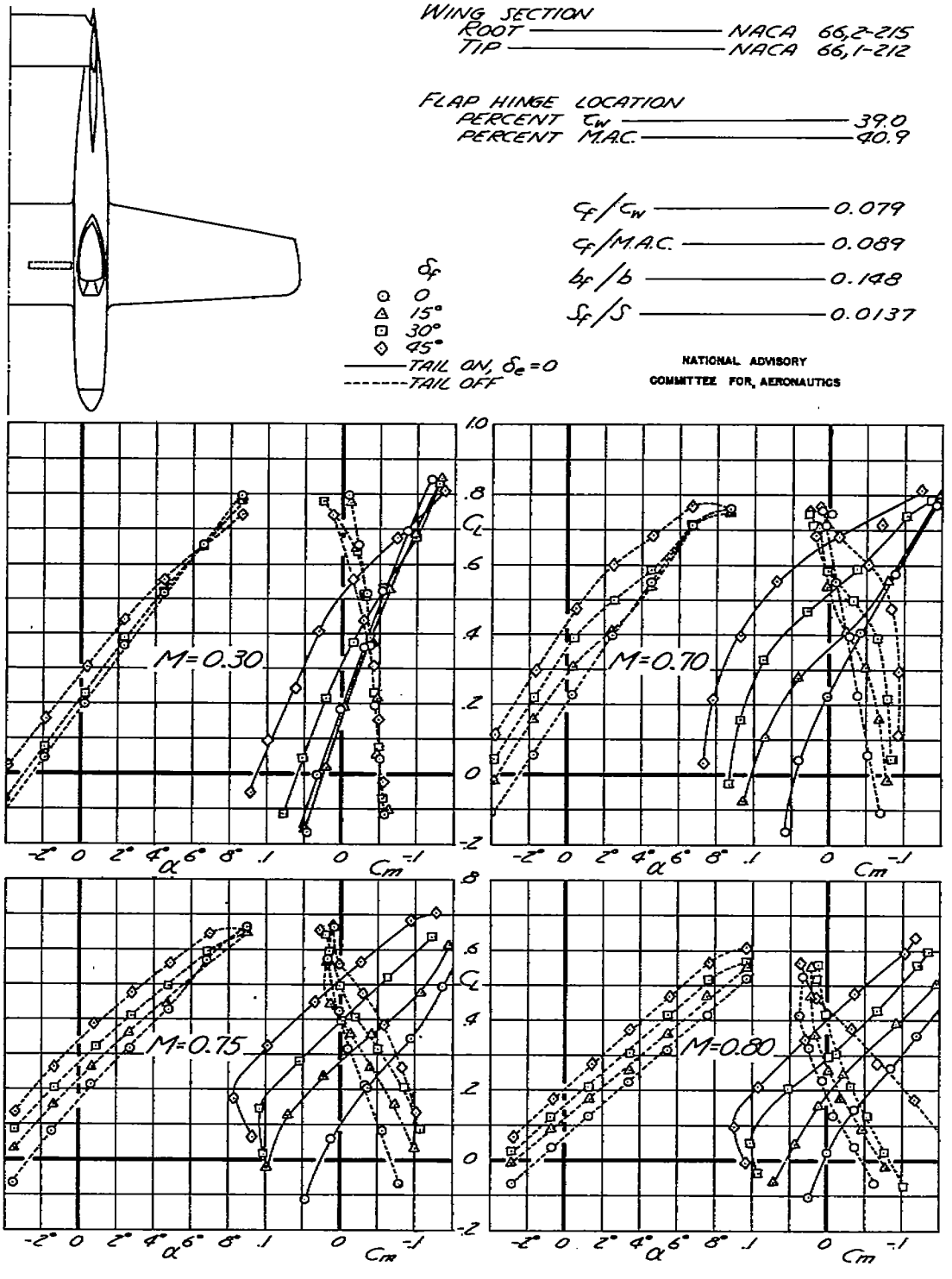

FIGURE 7.- EFFECT OF DIVE-RECOVERY FLAPS ON THE LIFT AND PITCHING-MOMENT CHARACTERISTICS OF THE NORTH AMERICAN XP-82 AIRPLANE MODEL.

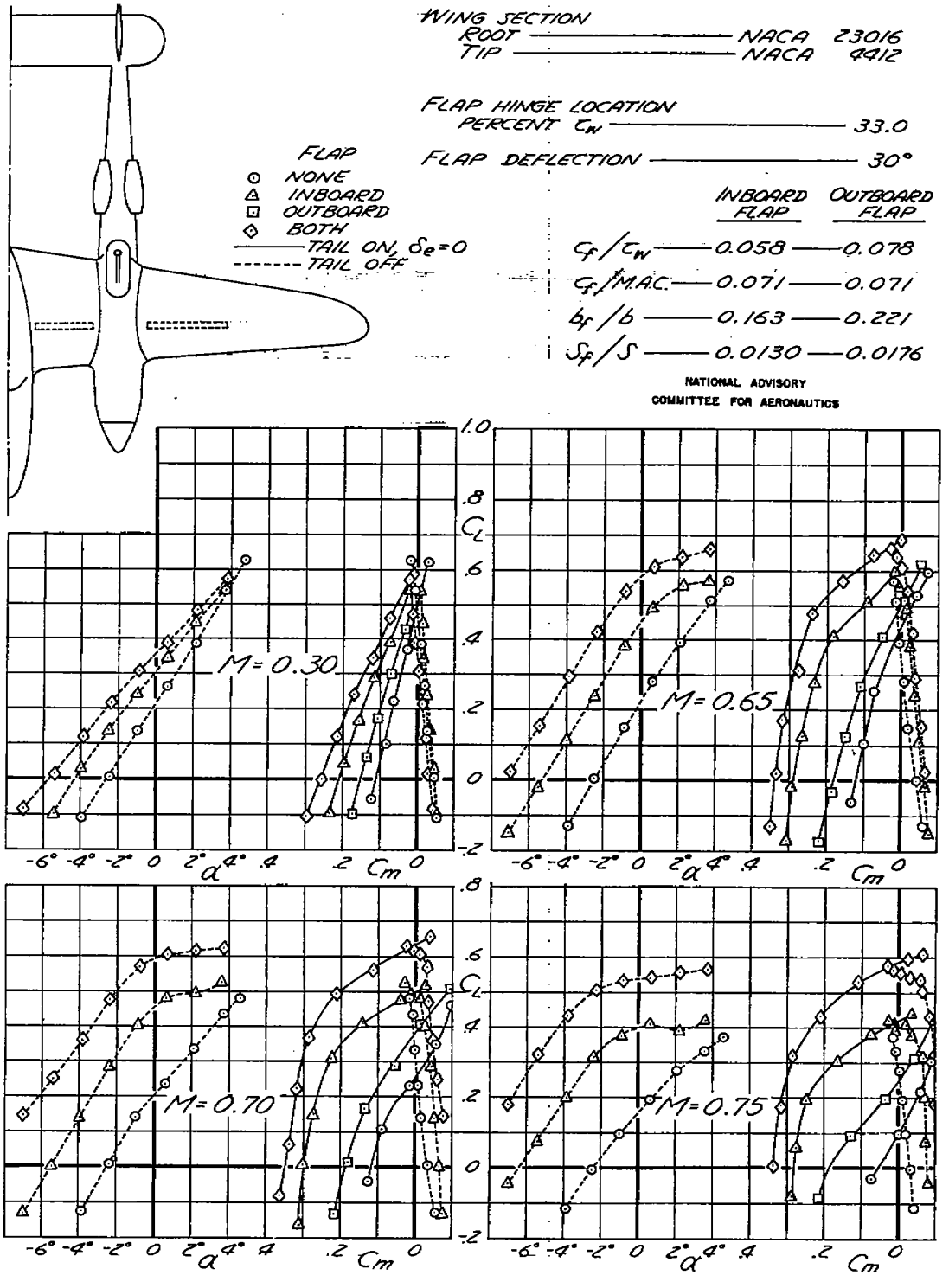

FIGURE 8.- EFFECT OF DIVE-RECOVERY FLAPS ON THE LIFT AND PITCHING-MOMENT CHARACTERISTICS OF THE LOCKHEED P-38 AIRPLANE MODEL.

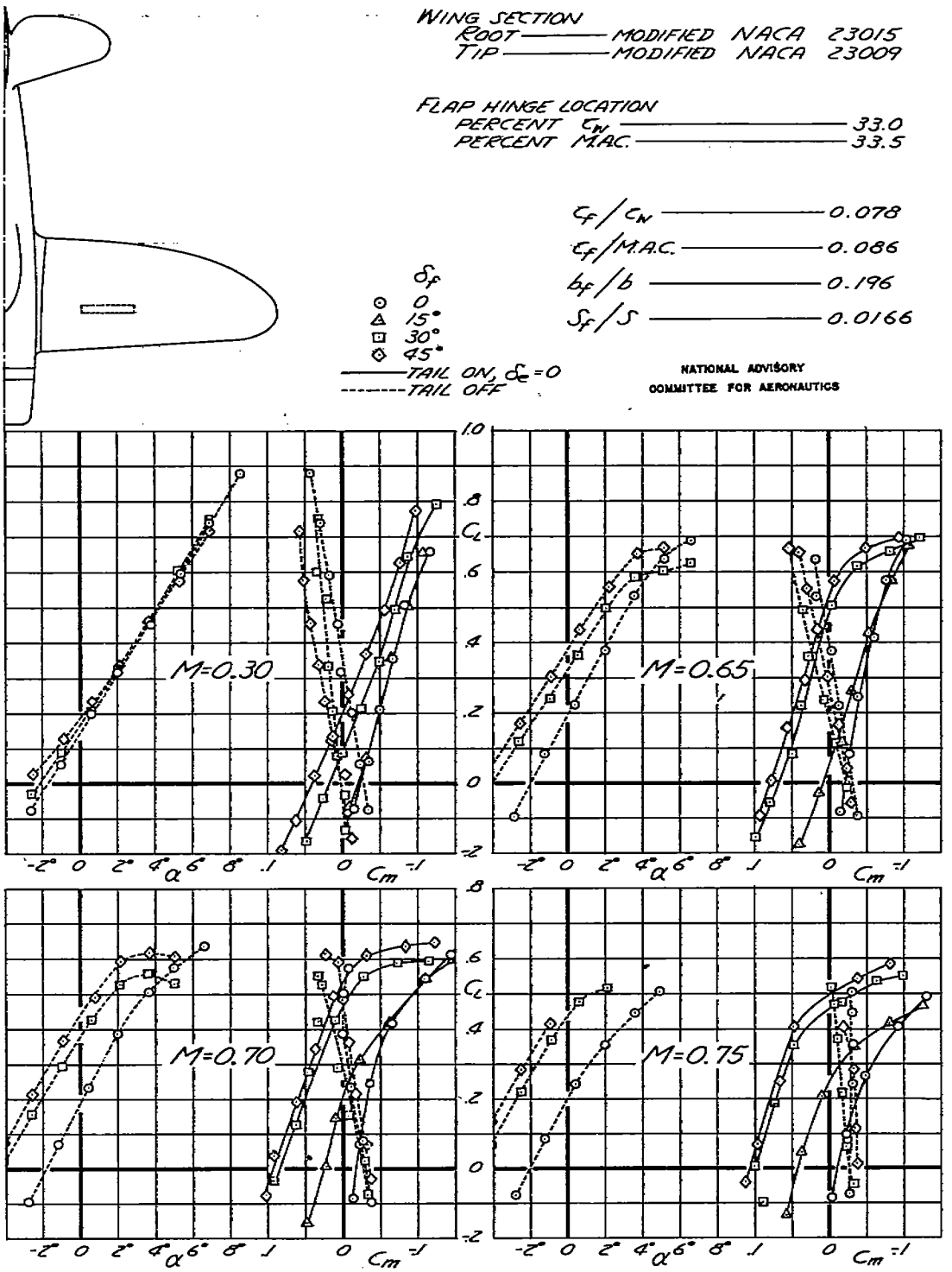

FIGURE 9. - EFFECT OF DIVE-RECOVERY FLAPS ON THE LIFT AND PITCHING-MOMENT CHARACTERISTICS OF THE REPUBLIC P-47D AIRPLANE MODEL.

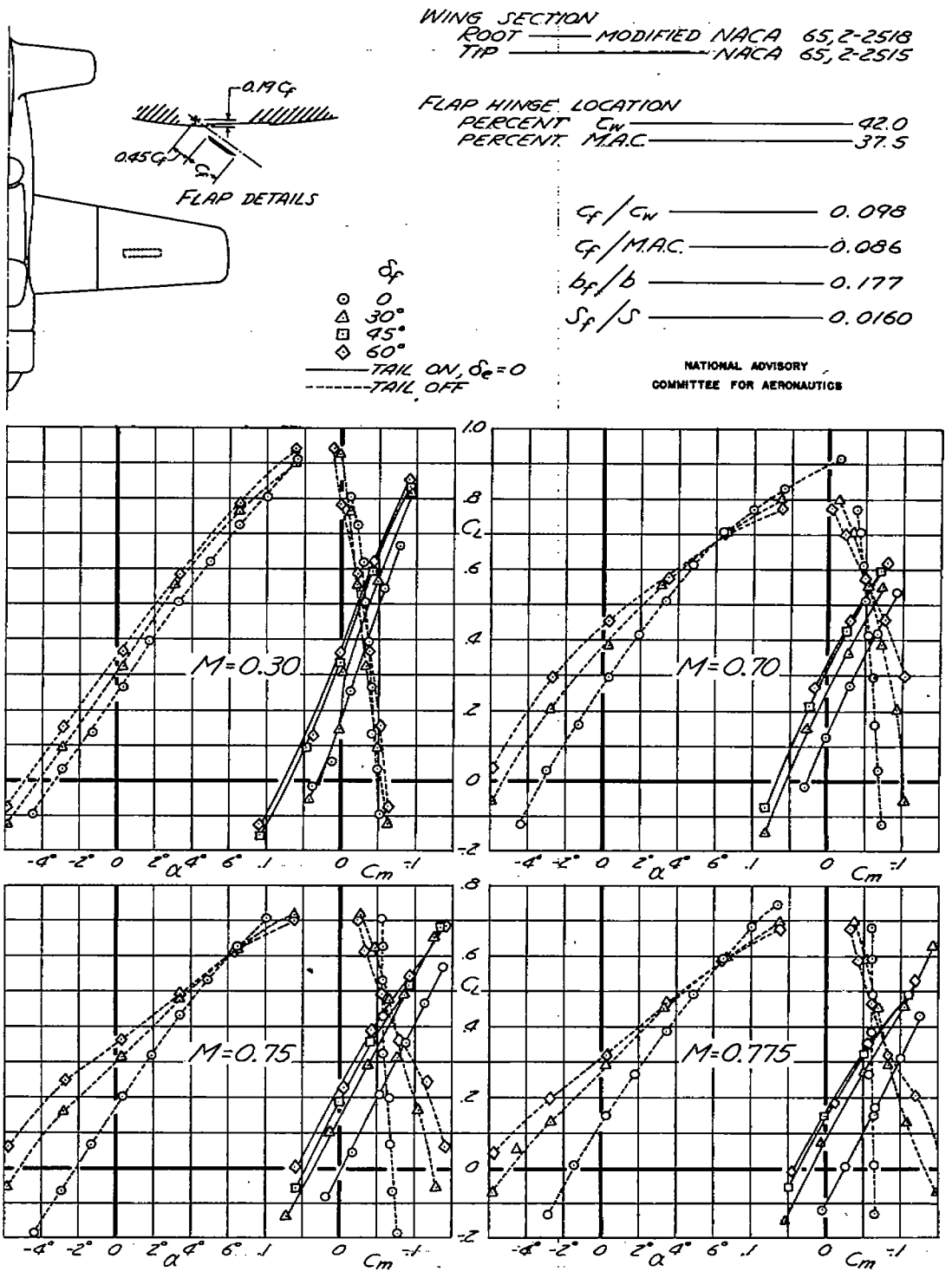

FIGURE 10. - EFFECT OF DIVE-RECOVERY FLAPS ON THE LIFT AND PITCHING-MOMENT CHARACTERISTICS OF THE DOUGLAS XSB2D-1 AIRPLANE MODEL.

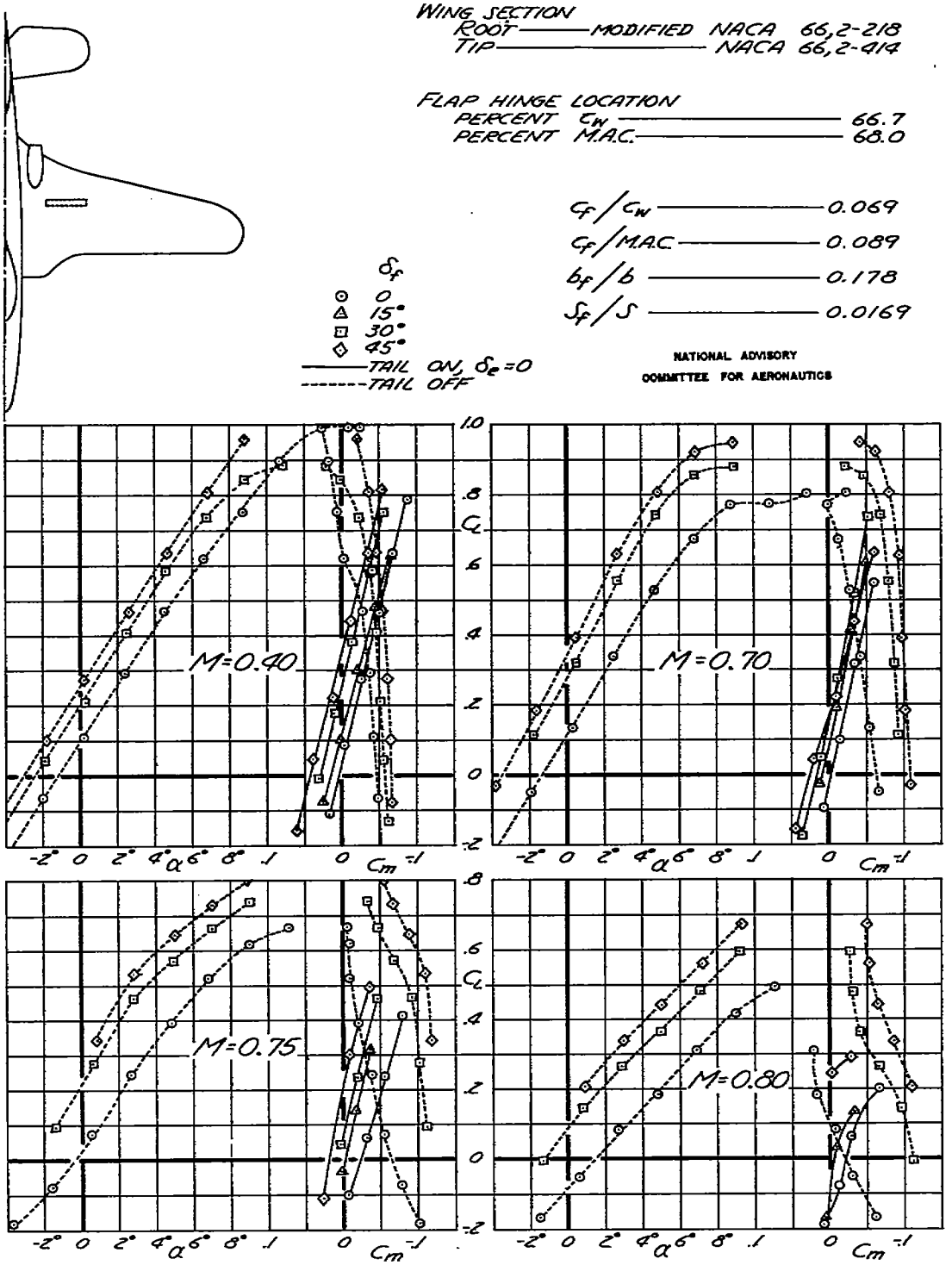

FIGURE 11.— EFFECT OF DIVE-RECOVERY FLAPS ON THE LIFT AND PITCHING-MOMENT CHARACTERISTICS OF THE McDONNELL XFD-1 AIRPLANE MODEL.

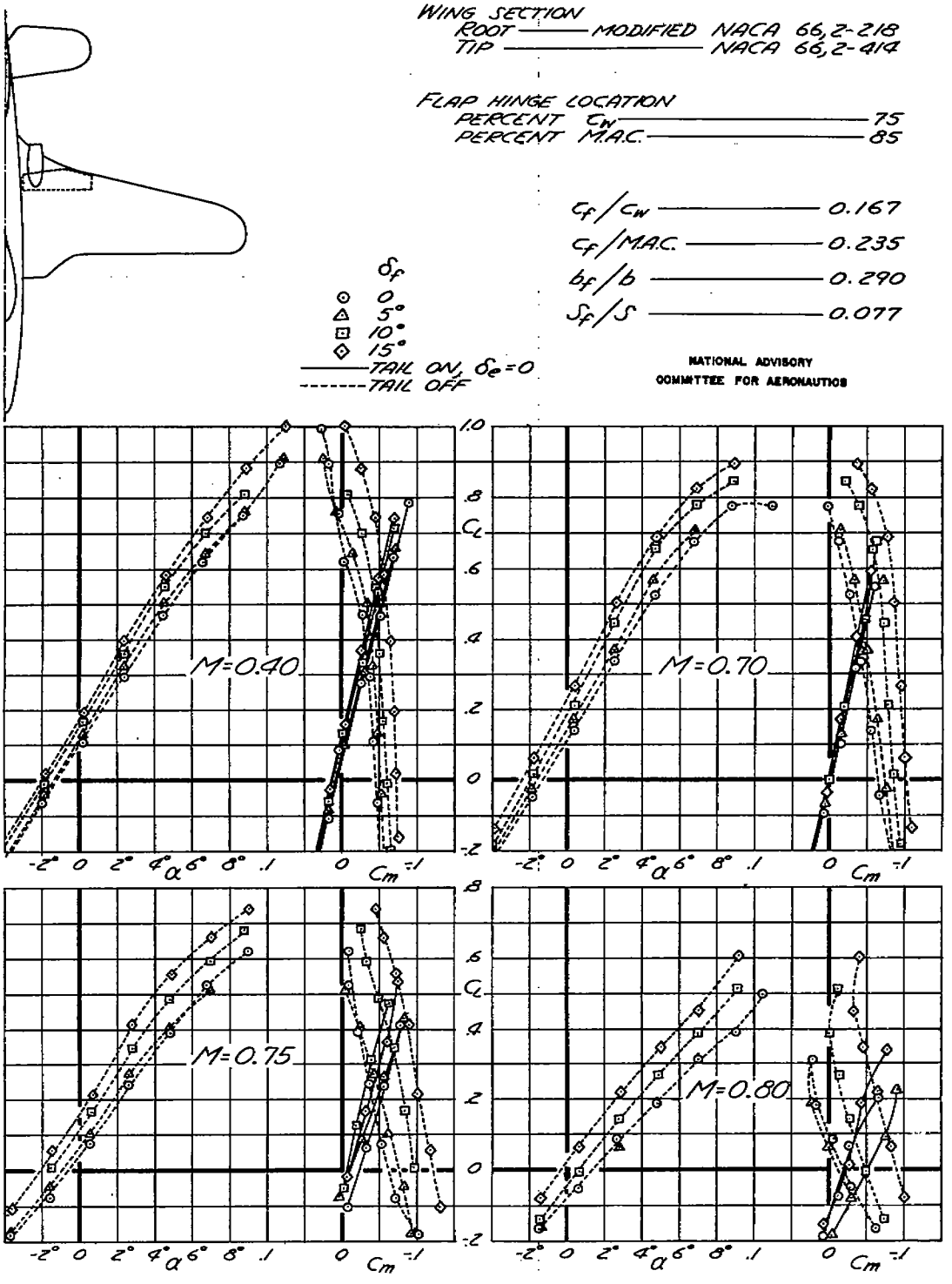

FIGURE 12.- EFFECT OF INBOARD LANDING FLAPS ON THE LIFT AND PITCHING-MOMENT CHARACTERISTICS OF THE McDONNELL XFD-1 AIRPLANE MODEL.

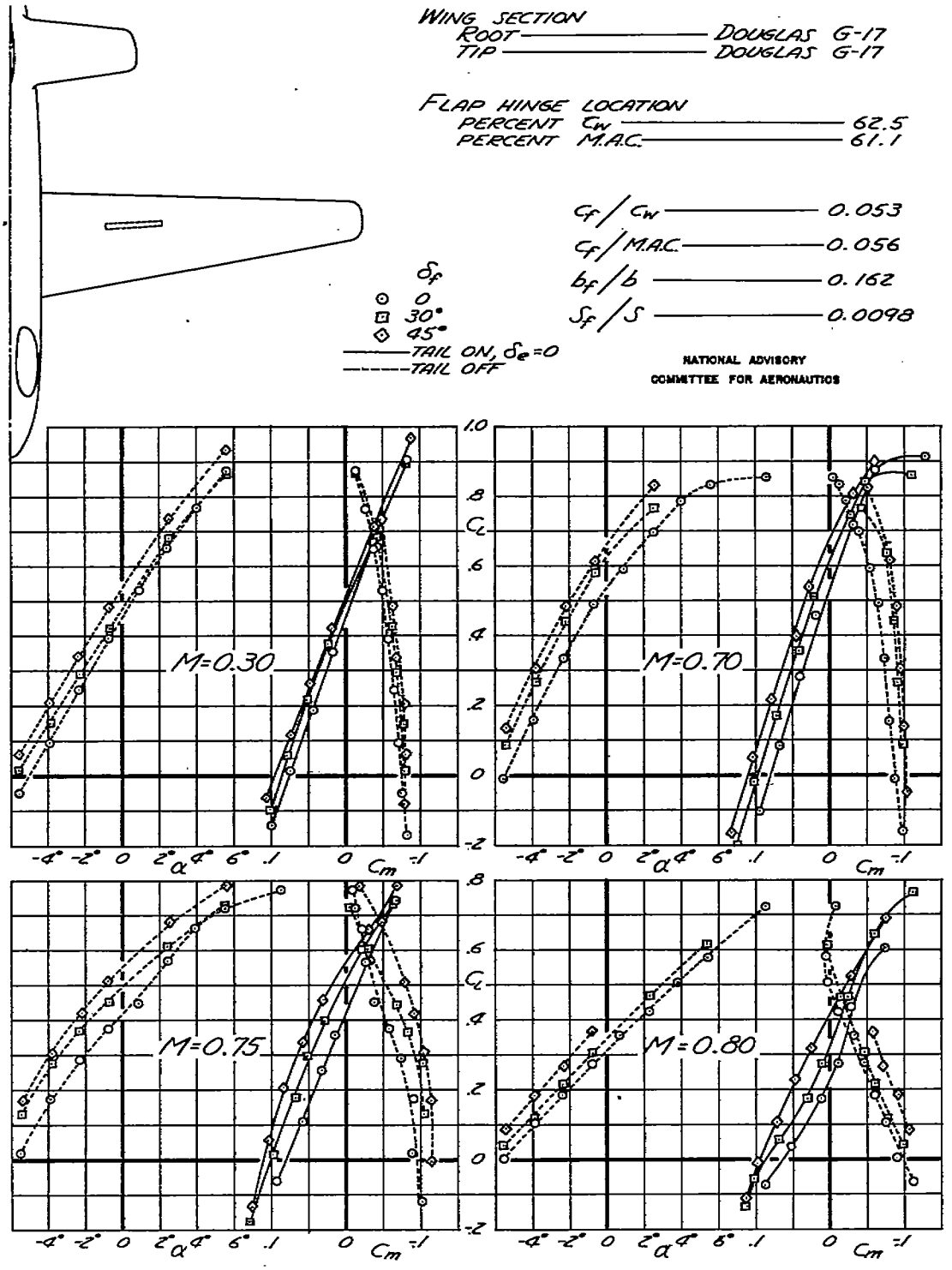

FIGURE 13.- EFFECT OF DIVE-RECOVERY FLAPS ON THE LIFT AND PITCHING-MOMENT CHARACTERISTICS OF THE DOUGLAS XB-42 AIRPLANE MODEL.

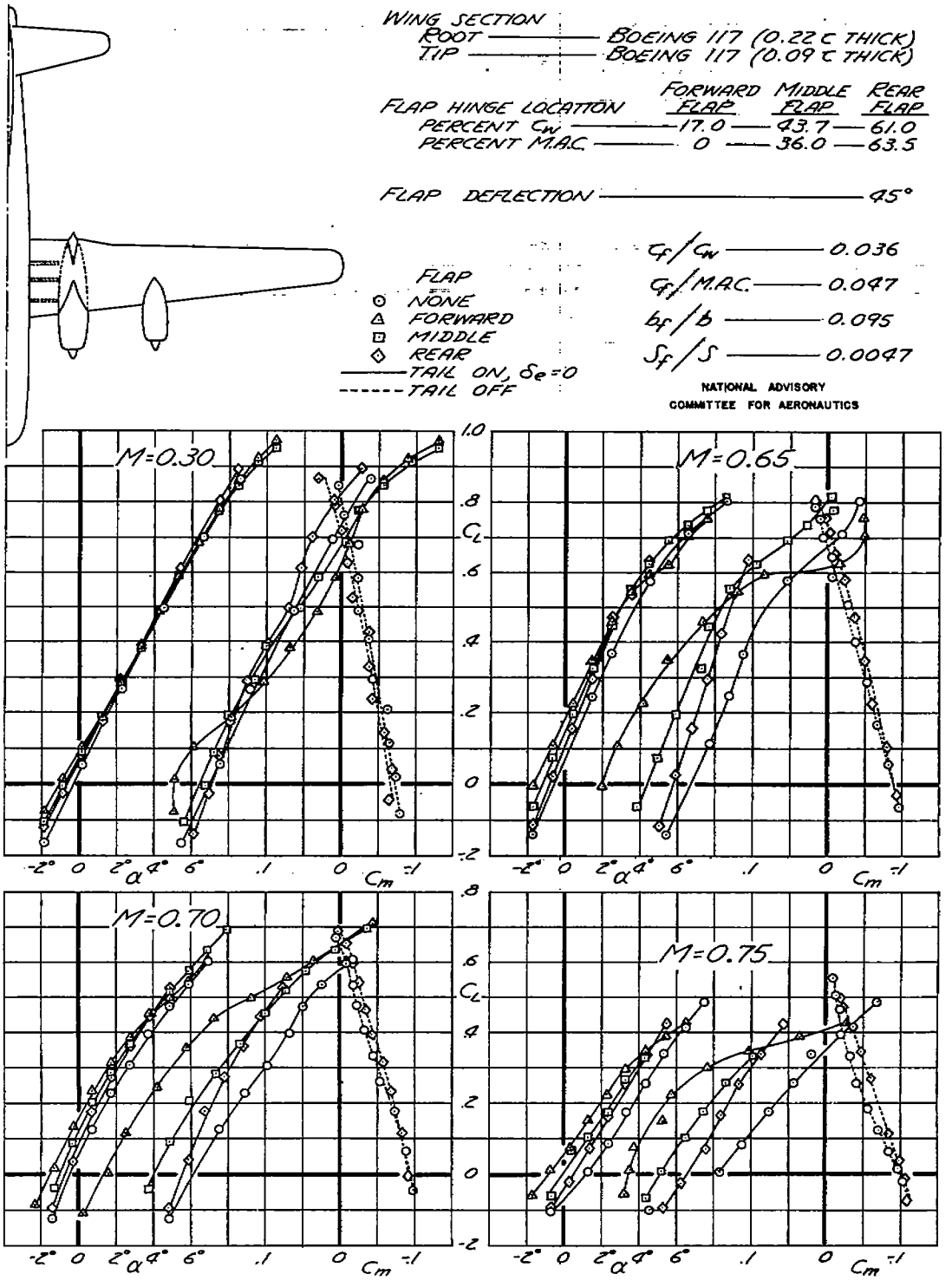

FIGURE 14. - EFFECT OF DIVE-RECOVERY FLAPS ON THE LIFT AND PITCHING-MOMENT CHARACTERISTICS OF THE BOEING XB-29 AIRPLANE MODEL.

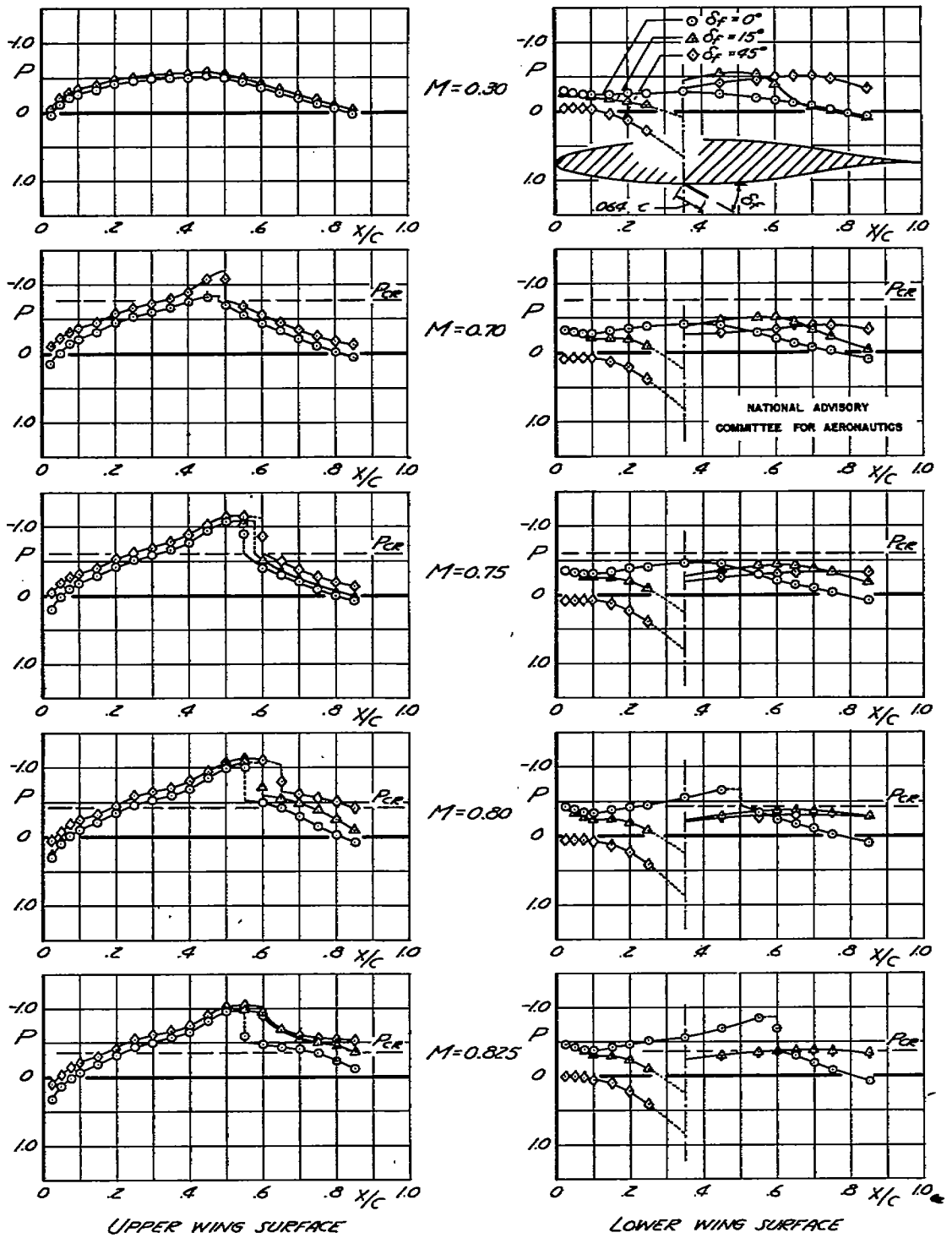

(a) $\alpha_u = -1°$

FIGURE 15.- CHORDWISE PRESSURE DISTRIBUTION ON THE LOCKHEED YP-80A AIRPLANE MODEL WING AT A SECTION THROUGH THE FLAP.

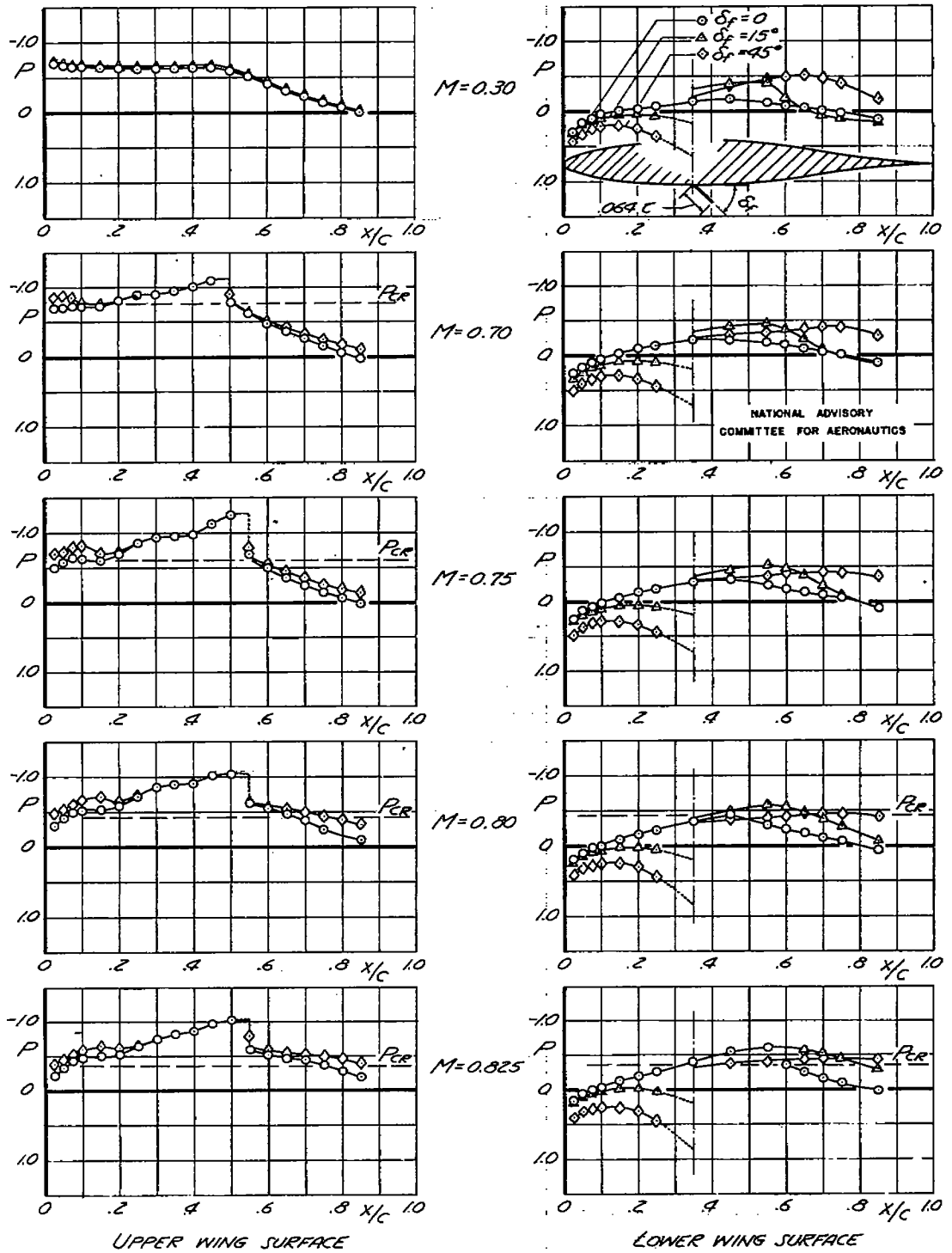

(b) $\alpha_U = +2°$

FIGURE 15.- (CONCLUDED)

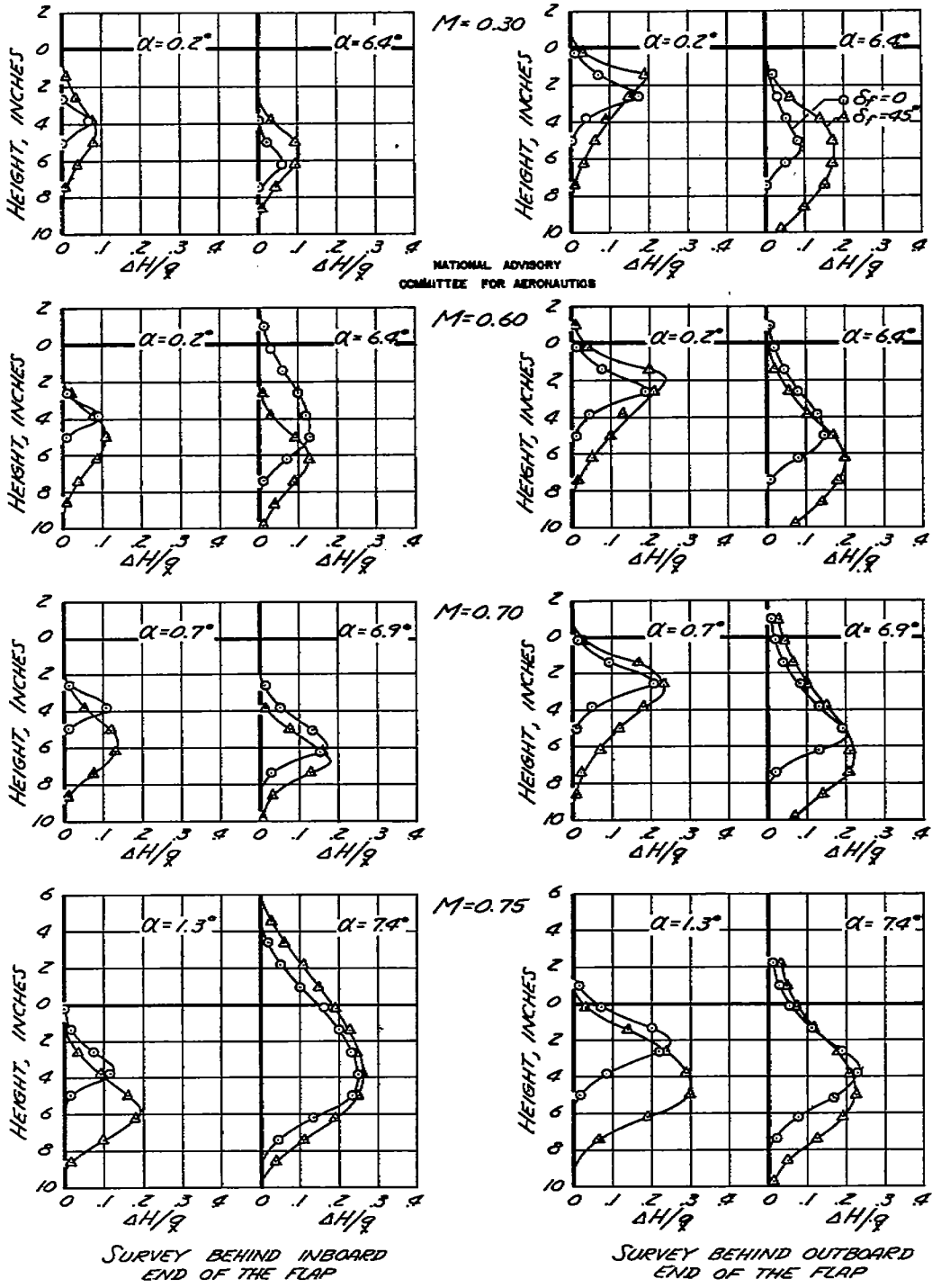

FIGURE 16.- EFFECT OF DIVE-RECOVERY FLAPS (AFT POSITION, REF. FIG. 14) ON THE WING WAKE AT THE TAIL OF THE BOEING XB-29 AIRPLANE MODEL.

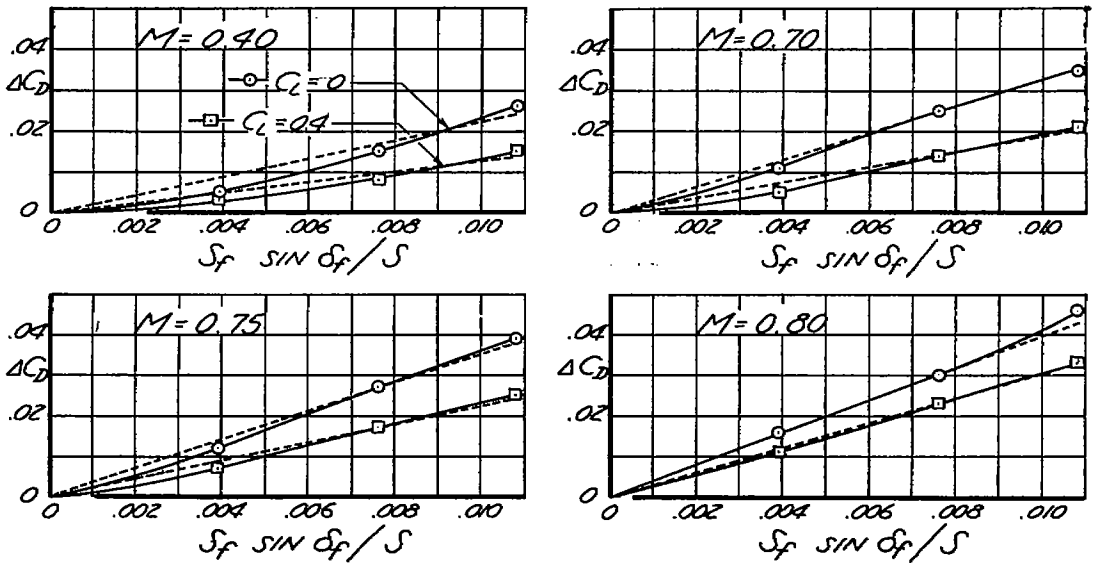

(a) TYPICAL VARIATION OF DRAG COEFFICIENT WITH PROJECTED FRONTAL AREA OF THE FLAP (XP-81 AIRPLANE MODEL)

NATIONAL ADVISORY COMMITTEE FOR AERONAUTICS

- XP-80 WITH 65-213 WING
- XP-80 WITH 66-416 to 66-616 WING
- YP-80A
- XP-81
- XP-82
- P-47D
- XSB2D-1
- XFD-1
- XB-42

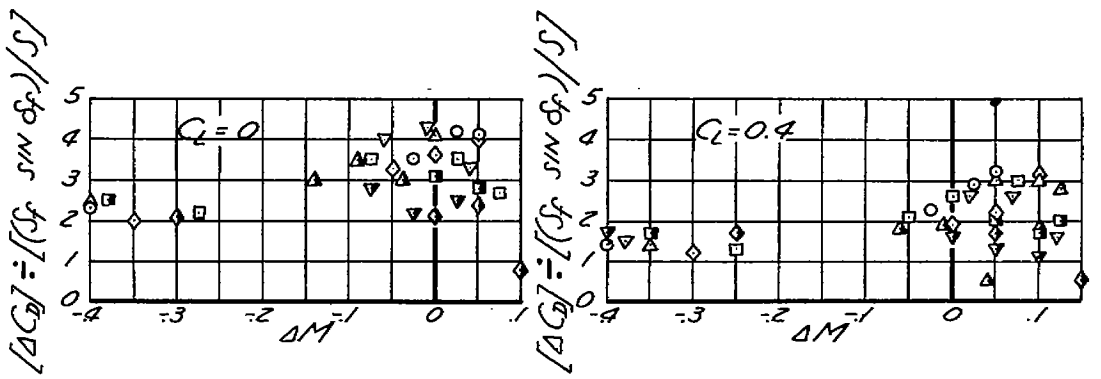

(b) THE DRAG COEFFICIENT DUE TO THE FLAPS ON SEVERAL MODELS AS A FUNCTION OF THE EXCESS OVER THE LIFT-DIVERGENCE MACH NUMBER

FIGURE 17.- THE EFFECT OF DIVE-RECOVERY FLAPS ON THE DRAG COEFFICIENT OF SEVERAL AIRPLANE MODELS.

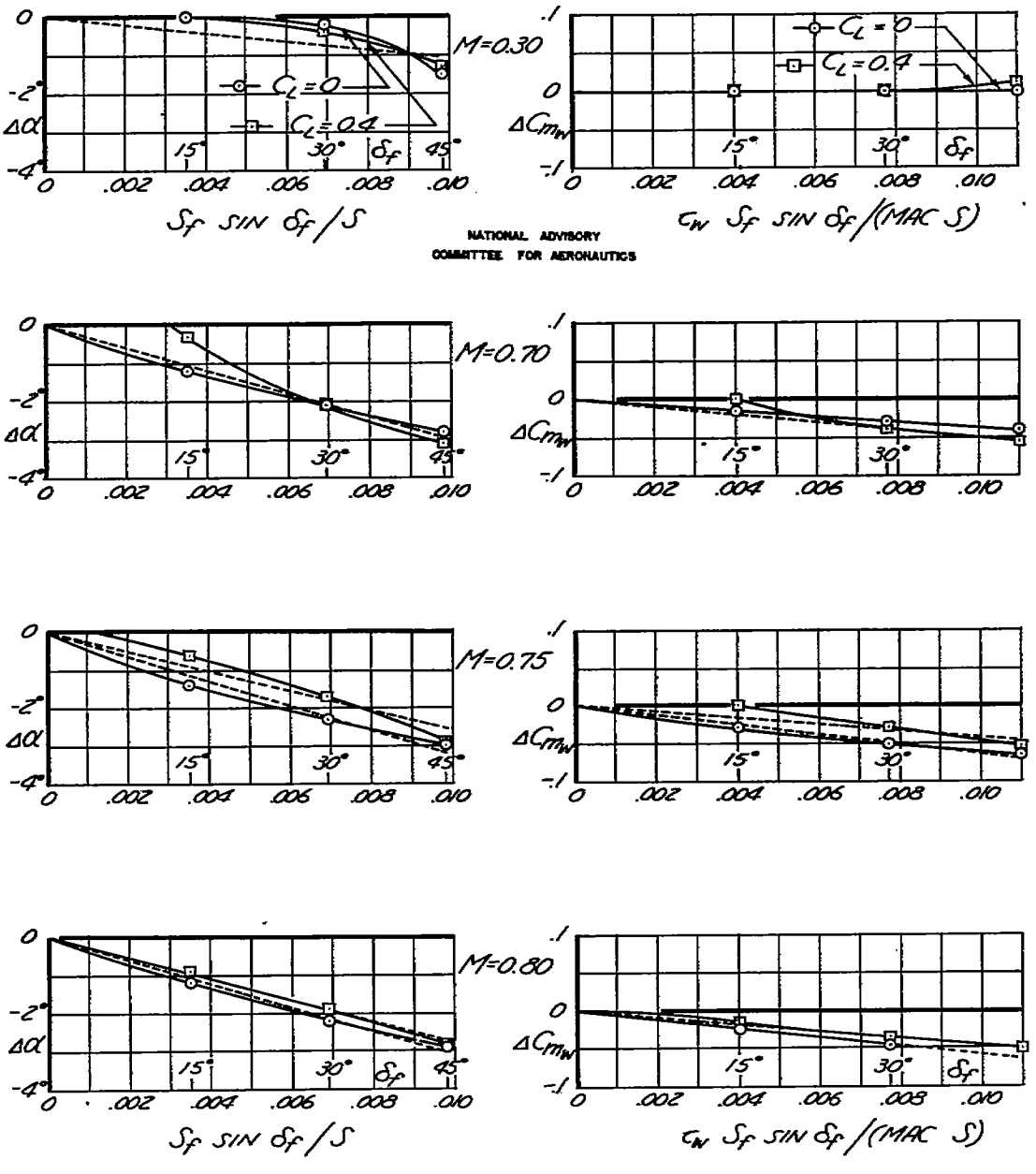

FIGURE 18.- TYPICAL VARIATION OF WING PITCHING-MOMENT COEFFICIENT AND ANGLE OF ATTACK FOR CONSTANT LIFT COEFFICIENT WITH PROJECTED FLAP FRONTAL AREA (XP-82 AIRPLANE MODEL).

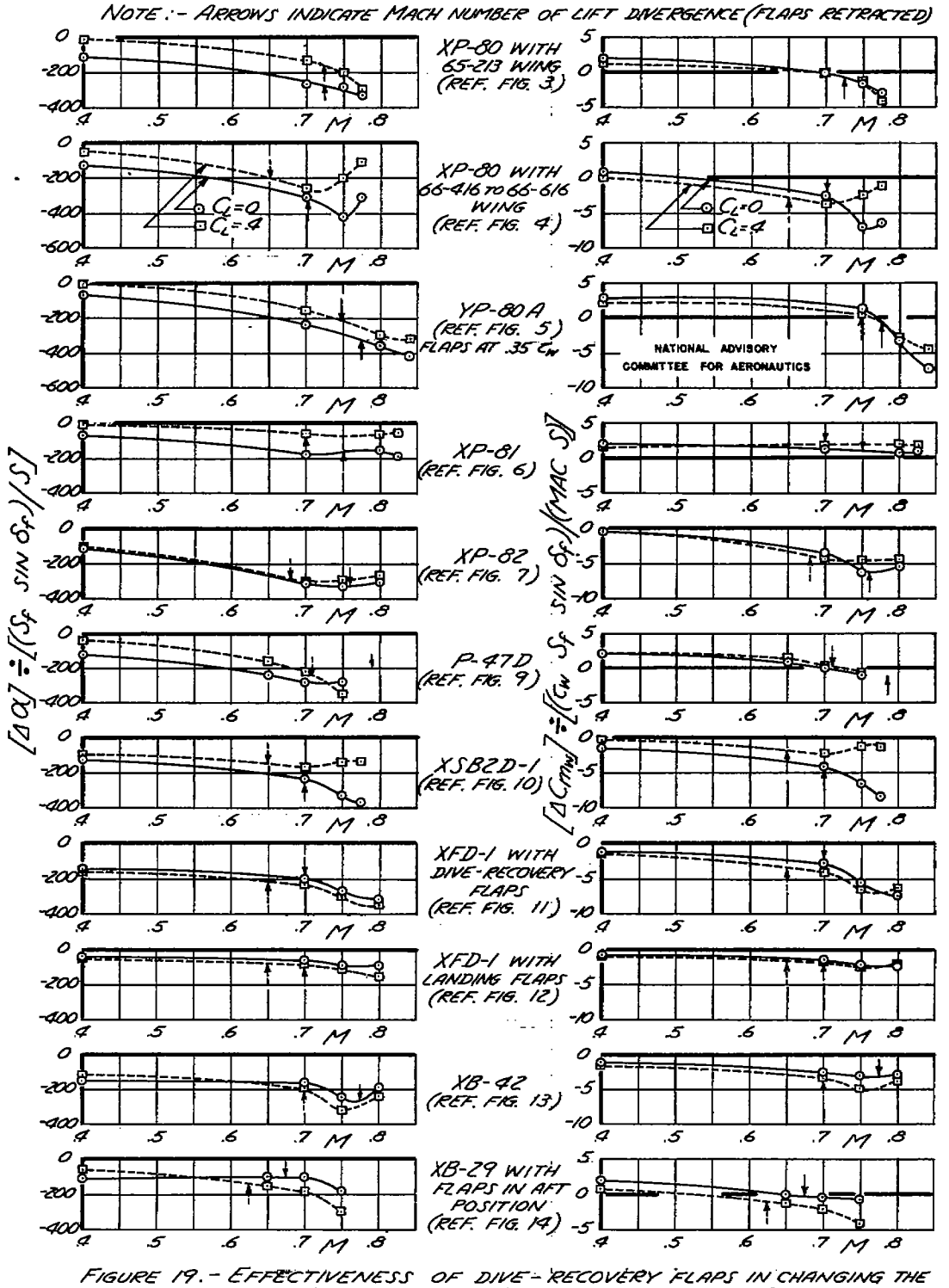

FIGURE 19.- EFFECTIVENESS OF DIVE-RECOVERY FLAPS IN CHANGING THE WING PITCHING-MOMENT COEFFICIENT AND ANGLE OF ATTACK FOR CONSTANT LIFT COEFFICIENT OF SEVERAL AIRPLANE MODELS AS A FUNCTION OF MACH NUMBER.

- ⊙ XP-80 WITH 65-213 WING (REF. FIG. 3)
- △ XP-80 WITH 66-416 TO 66-616 WING (REF. FIG. 4)
- ⊡ YP-80A (REF. FIG. 5)
- ◇ XP-81 (REF. FIG. 6)
- ▽ XP-82 (REF. FIG. 7)
- ◐ P-38 (REF. FIG. 8)
- ▲ P-47D (REF. FIG. 9)
- ◧ XSB2D-1 (REF. FIG. 10)
- ◆ XFD-1 (REF. FIG. 11)
- ▼ XB-42 (REF. FIG. 13)
- × XB-29 (REF. FIG. 14)

NATIONAL ADVISORY
COMMITTEE FOR AERONAUTICS

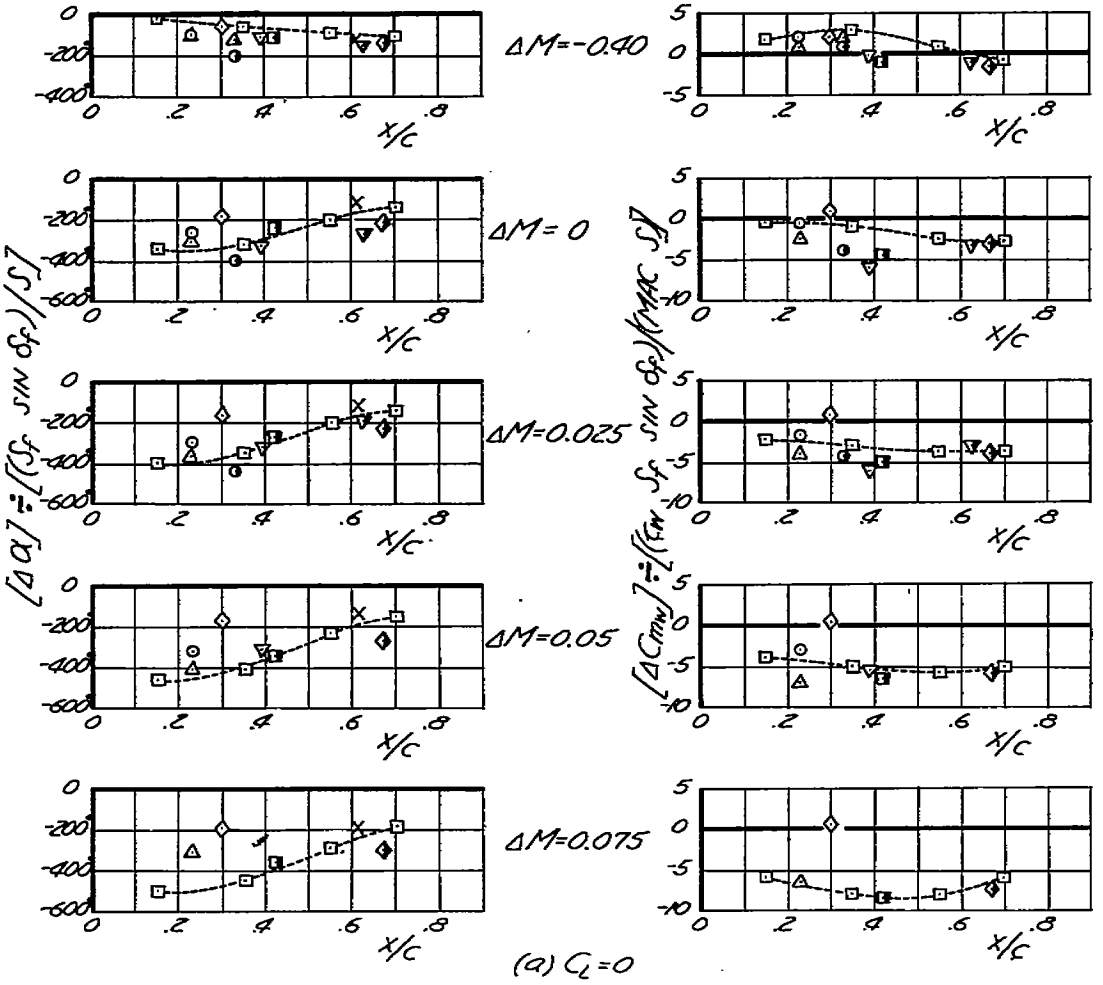

(a) $C_L = 0$

FIGURE 20.- EFFECTIVENESS OF DIVE-RECOVERY FLAPS IN CHANGING THE WING PITCHING-MOMENT COEFFICIENT AND ANGLE OF ATTACK FOR CONSTANT LIFT COEFFICIENT OF SEVERAL AIRPLANE MODELS AS A FUNCTION OF CHORDWISE POSITION OF THE FLAPS.

⊙ XP-80 WITH 65-213 WING (REF. FIG. 3)
△ XP-80 WITH 66-416 TO 66-616 WING (REF. FIG. 4)
□ YP-80A (REF. FIG. 5)
◇ XP-81 (REF. FIG. 6)
▽ XP-82 (REF. FIG. 7)
◐ P-38 (REF. FIG. 8)
▲ P-47D (REF. FIG. 9)
◨ XSB2D-1 (REF. FIG. 10)
◆ XFD-1 (REF. FIG. 11)
▼ XB-42 (REF. FIG. 13)
× XB-29 (REF. FIG. 14)

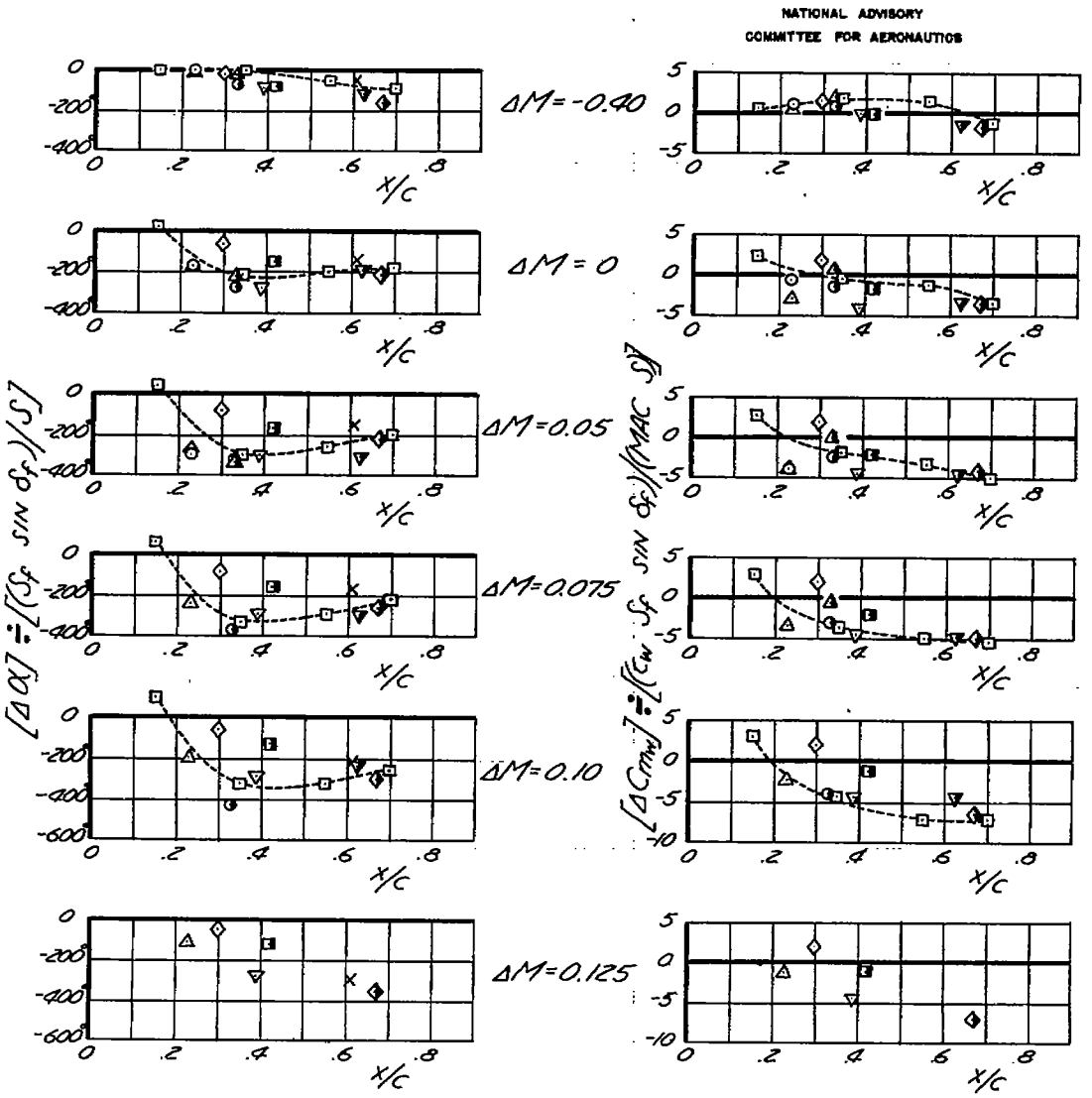

(b) $C_L = 0.40$

FIGURE 20.- (CONCLUDED)

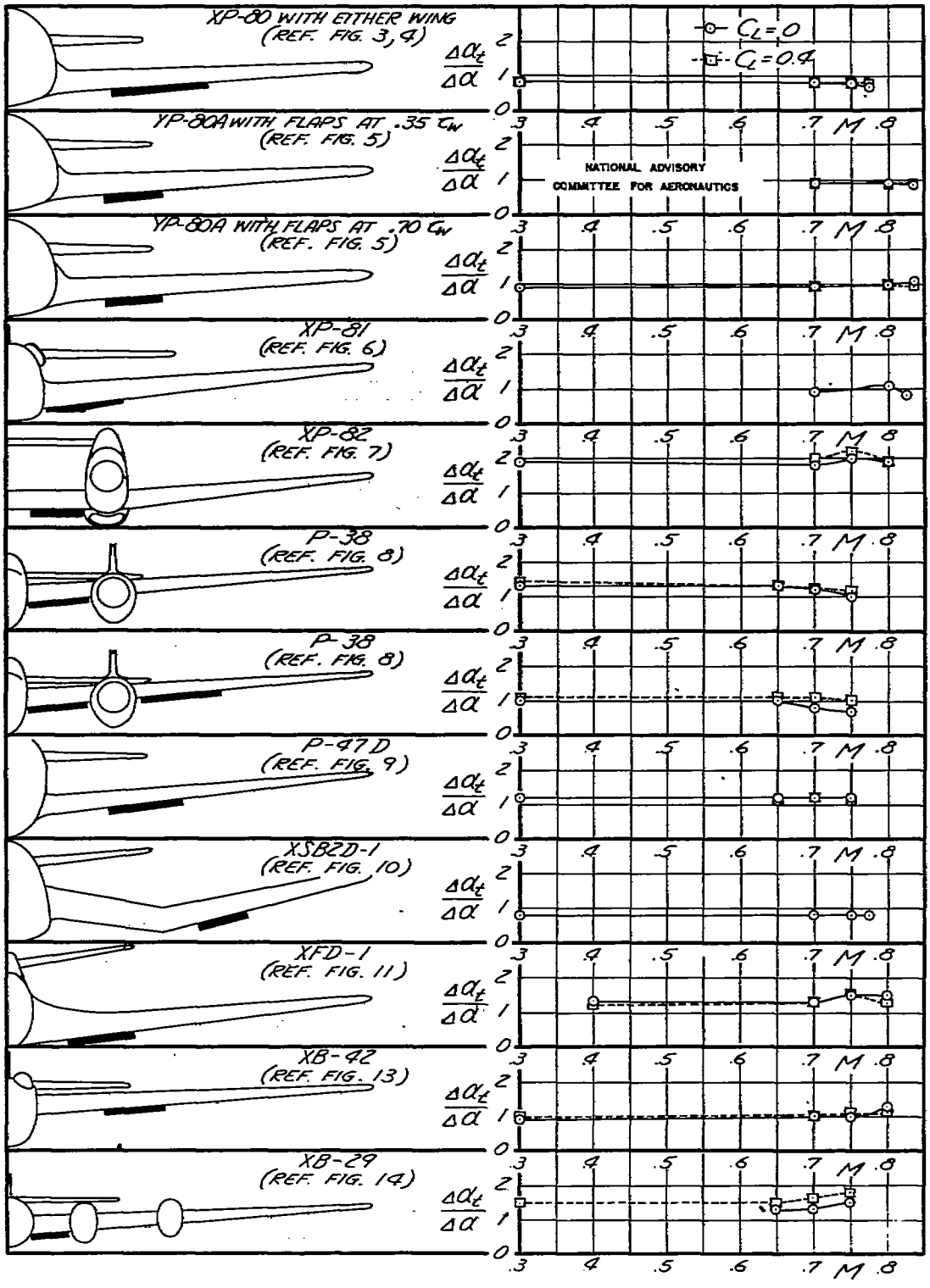

FIGURE 21.- EFFECTIVENESS OF DIVE-RECOVERY FLAPS IN CHANGING THE TAIL ANGLE OF ATTACK OF SEVERAL AIRPLANE MODELS.

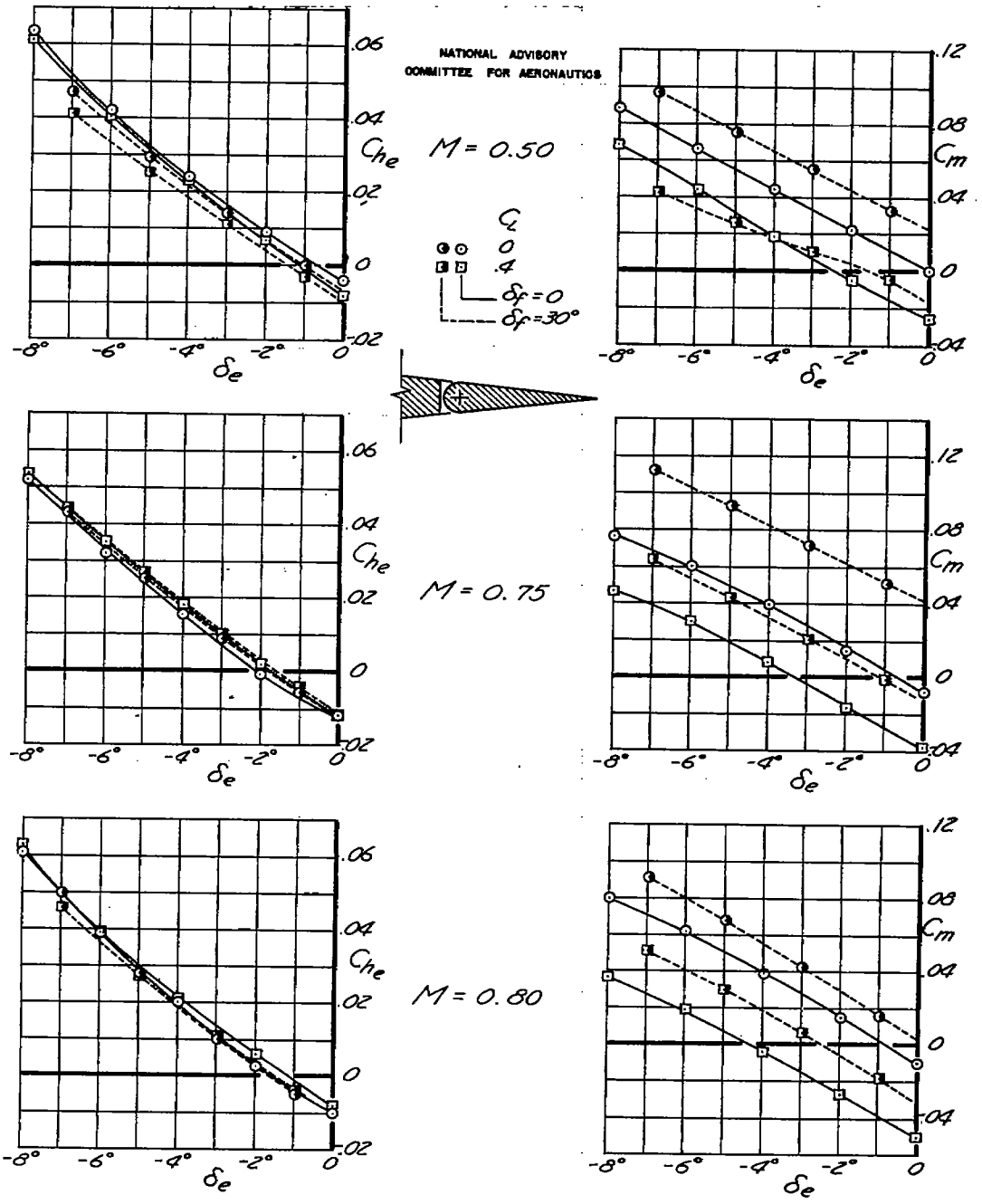

FIGURE 22.- THE EFFECT OF DIVE-RECOVERY FLAPS ON THE ELEVATOR CHARACTERISTICS OF THE LOCKHEED YP-80A AIRPLANE MODEL.

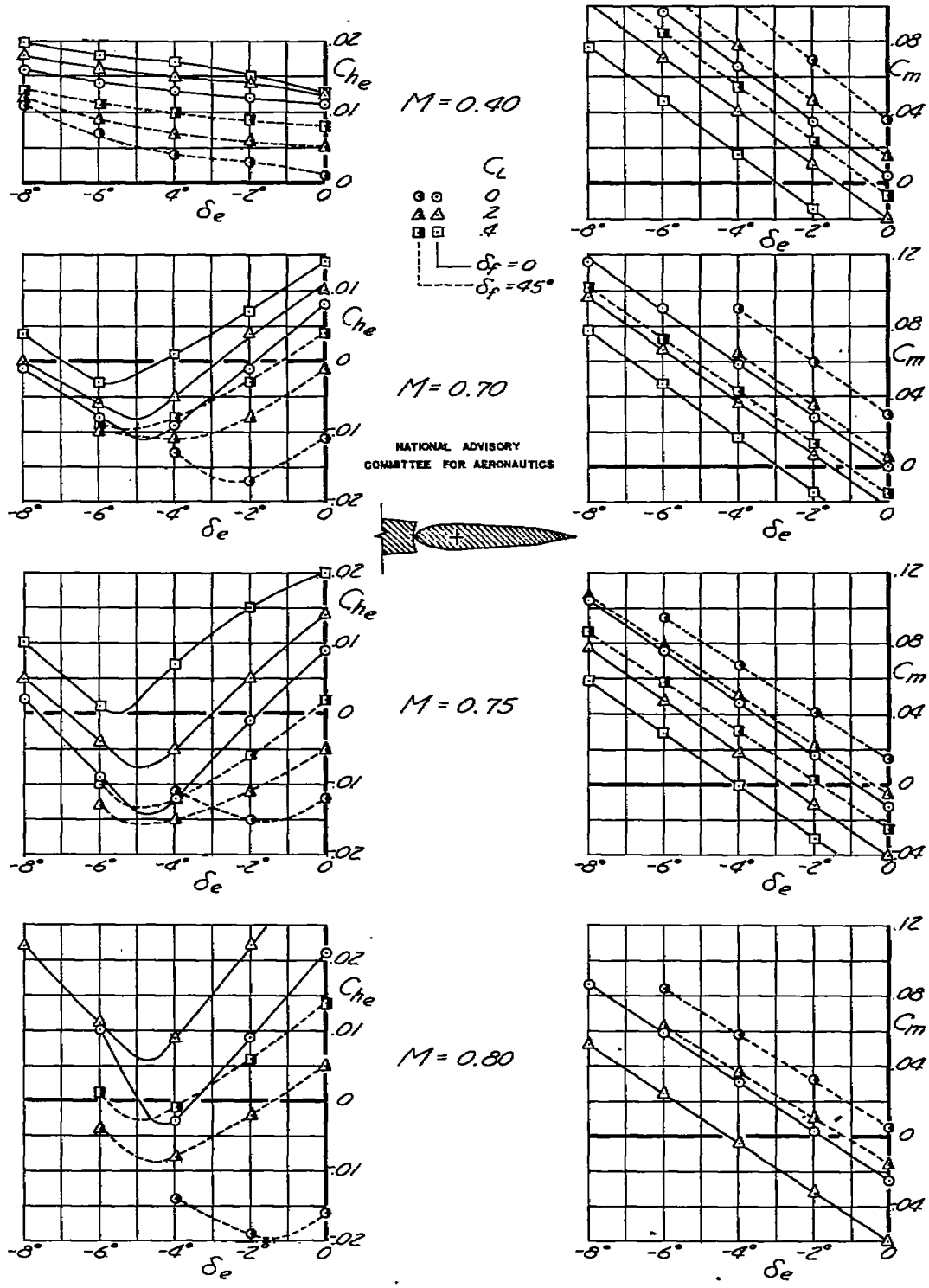

FIGURE 23.- THE EFFECT OF DIVE-RECOVERY FLAPS ON THE ELEVATOR CHARACTERISTICS OF THE McDONNELL XFD-1 AIRPLANE MODEL.

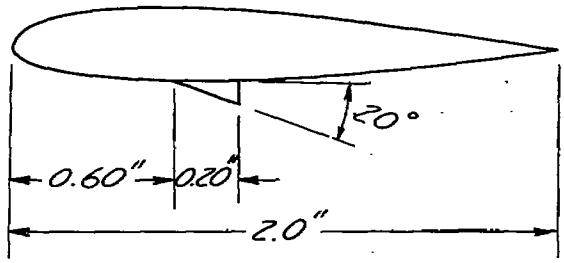

SECTION OF THE 2-INCH CHORD, 4-INCH SPAN MODEL WHICH WAS MOUNTED IN THE HIGH-SPEED-FLOW REGION OF AN AIRPLANE WING IN FLIGHT.

NATIONAL ADVISORY
COMMITTEE FOR AERONAUTICS

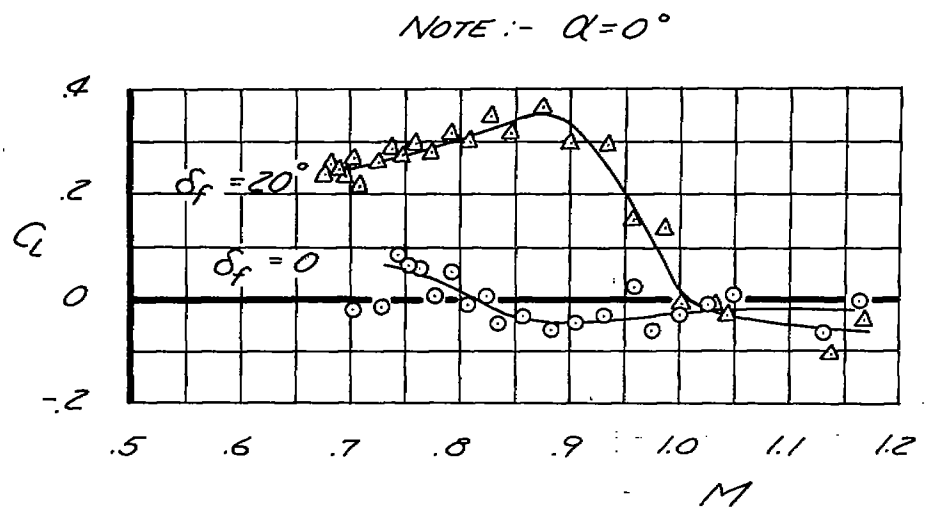

FIGURE 24.- EFFECT OF DIVE-RECOVERY FLAP ON THE LIFT CHARACTERISTICS OF A SMALL NACA 23015 AIRFOIL IN THE TRANSONIC SPEED RANGE.

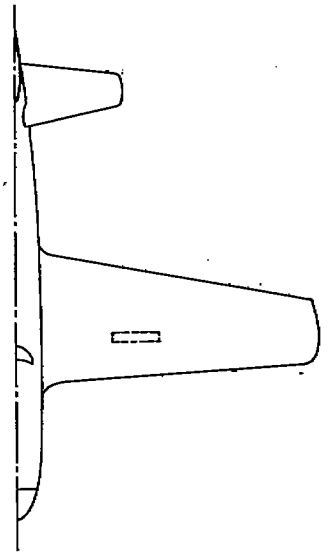

FLAP HINGE LOCATION
PERCENT C_w ——— 31.7
PERCENT M.A.C. ——— 27.5

c_f/c_w ——— 0.104
c_f/M.A.C ——— 0.094
b_f/b ——— 0.135
S_f/S ——— 0.0124

NATIONAL ADVISORY
COMMITTEE FOR AERONAUTICS

NOTE:- ALTITUDE = 20,000 FT.

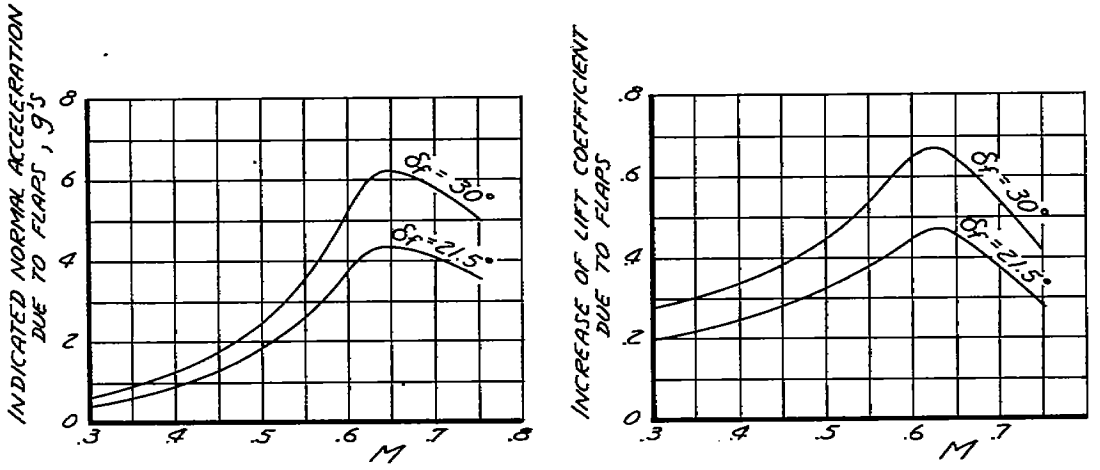

FIGURE 25.- THE ACCELERATION AND LIFT COEFFICIENT AVAILABLE FROM DIVE-RECOVERY FLAPS ON THE NORTH AMERICAN XP-51 AIRPLANE (RESULTS OF FLIGHT TESTS)